Space-based Wide-field Slitless Spectroscopy and Near-Ultraviolet Imaging

Xin Wang

UCAS/NAOC

Nov. 10, 2022

Department of Astronomy, Tsinghua University

Part I: Space-based Wide-field Slitless Spectroscopy

Part II: Space-based Near-Ultraviolet Imaging

Part III: Prospect for our CSST Main Survey

Space Telescopes Equipped with Slitless Spectroscopy

HST (1990, 2.4m)

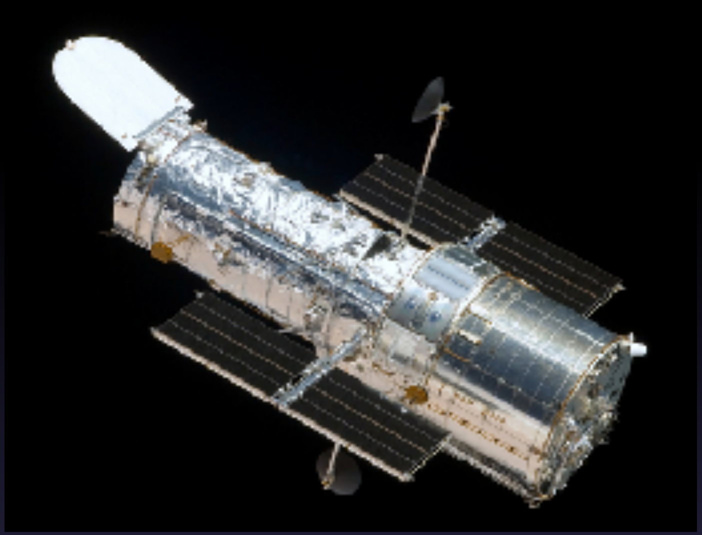

JWST (2021, 6.5m)

EUCLID (>2023, 1.2m)

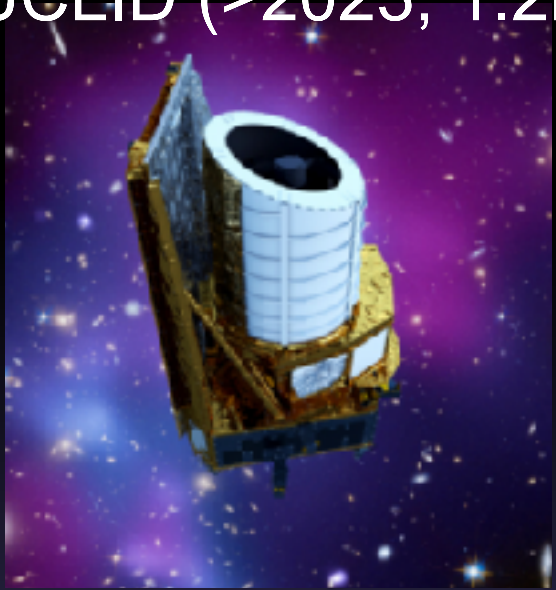

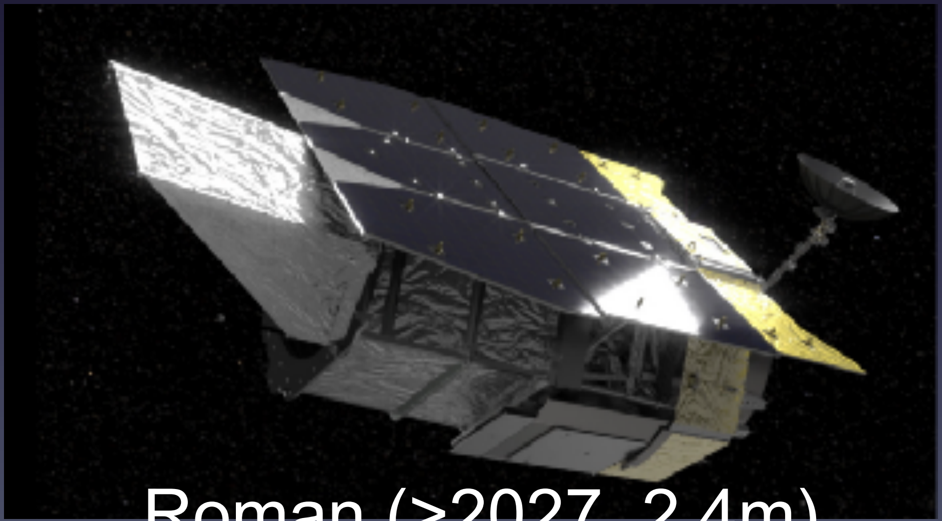

Roman (>2027, 2.4m)

CSST (~2024, 2m)

The concept of wide-field grism slitless spectroscopy

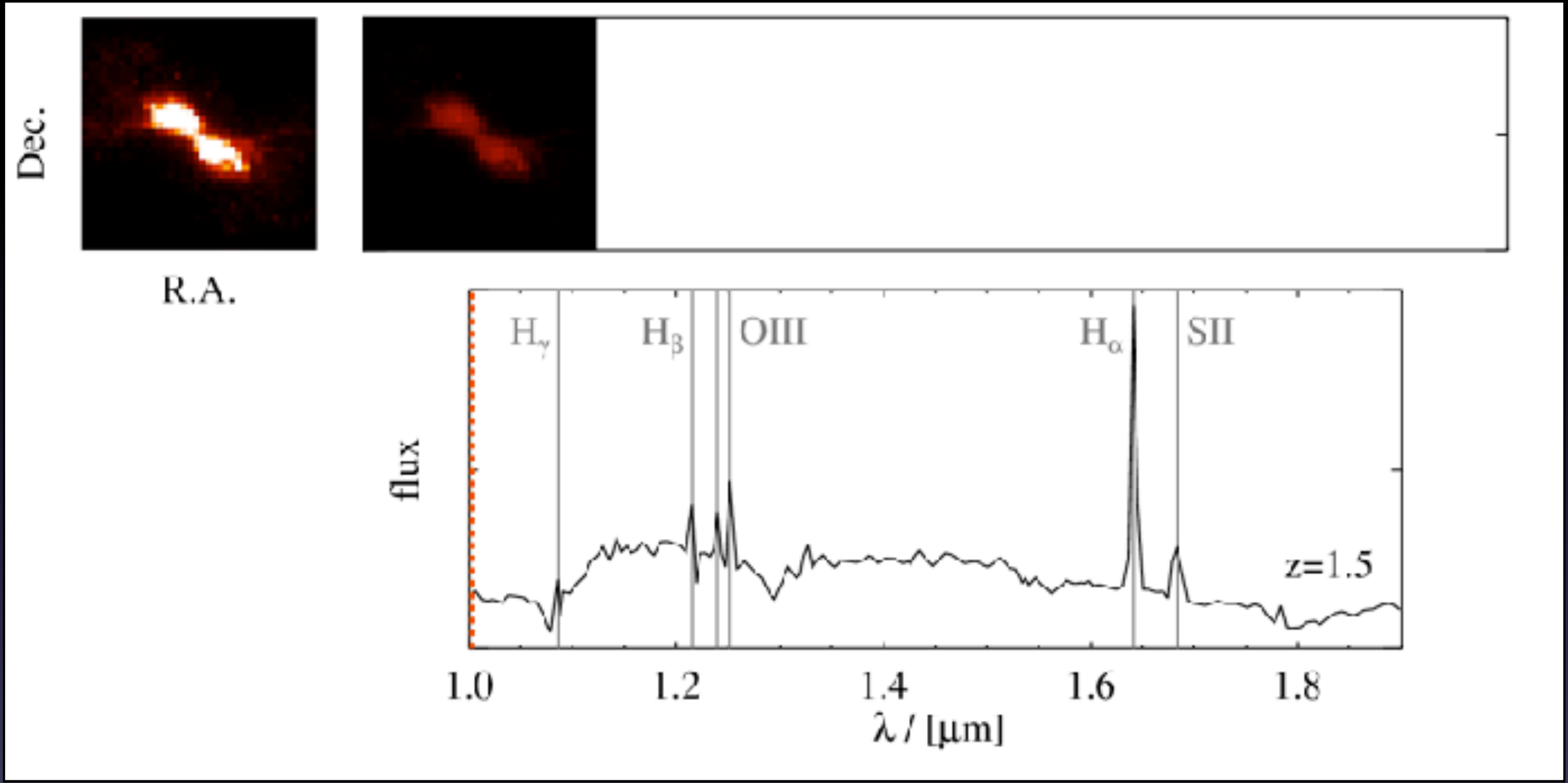

- Horizontal direction: wavelength dispersion convolved with source morphology.
- Vertical direction: spatial information.

MACS 1149 (HFF/GLASS cluster)

Direct imaging

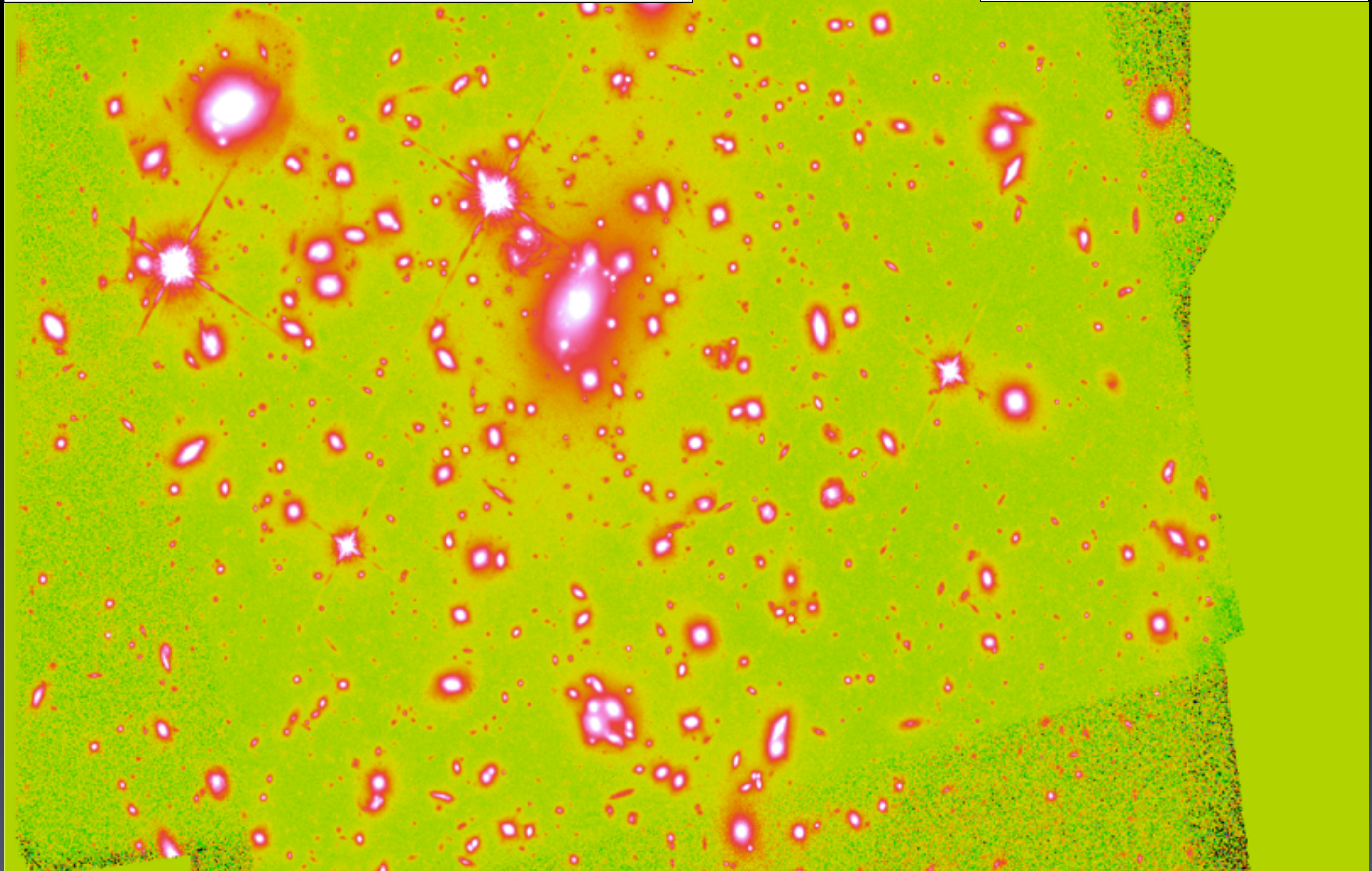

Wang et al. (2017) arXiv:1610.07558
Wang et al. (2019) arXiv:1808.08800
Wang et al. (2020) arXiv:1911.09841

MACS 1149 (HFF/GLASS cluster)

G141 *Model*

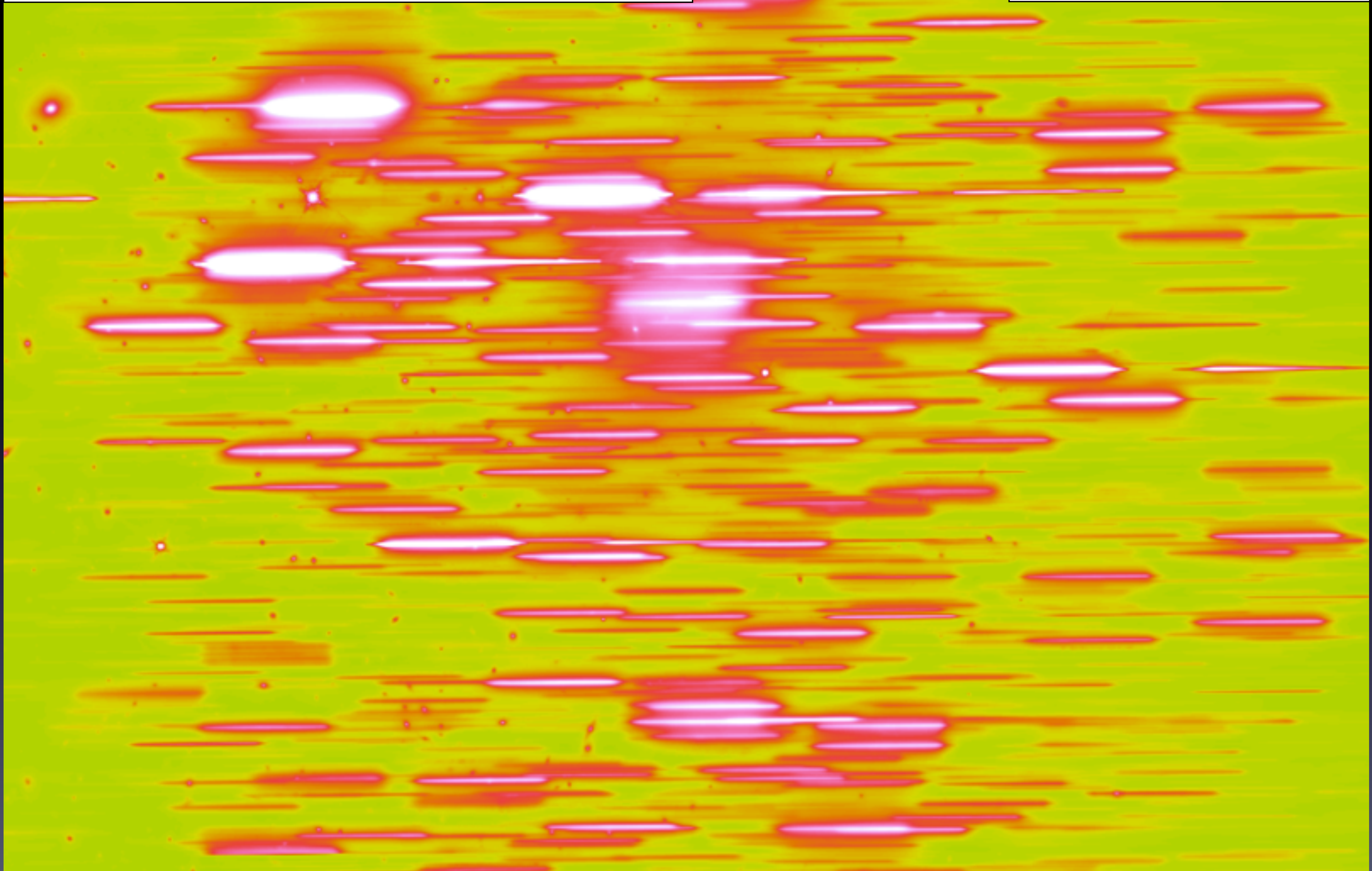

Wang et al. (2017) arXiv:1610.07558

Wang et al. (2019) arXiv:1808.08800

Wang et al. (2020) arXiv:1911.09841

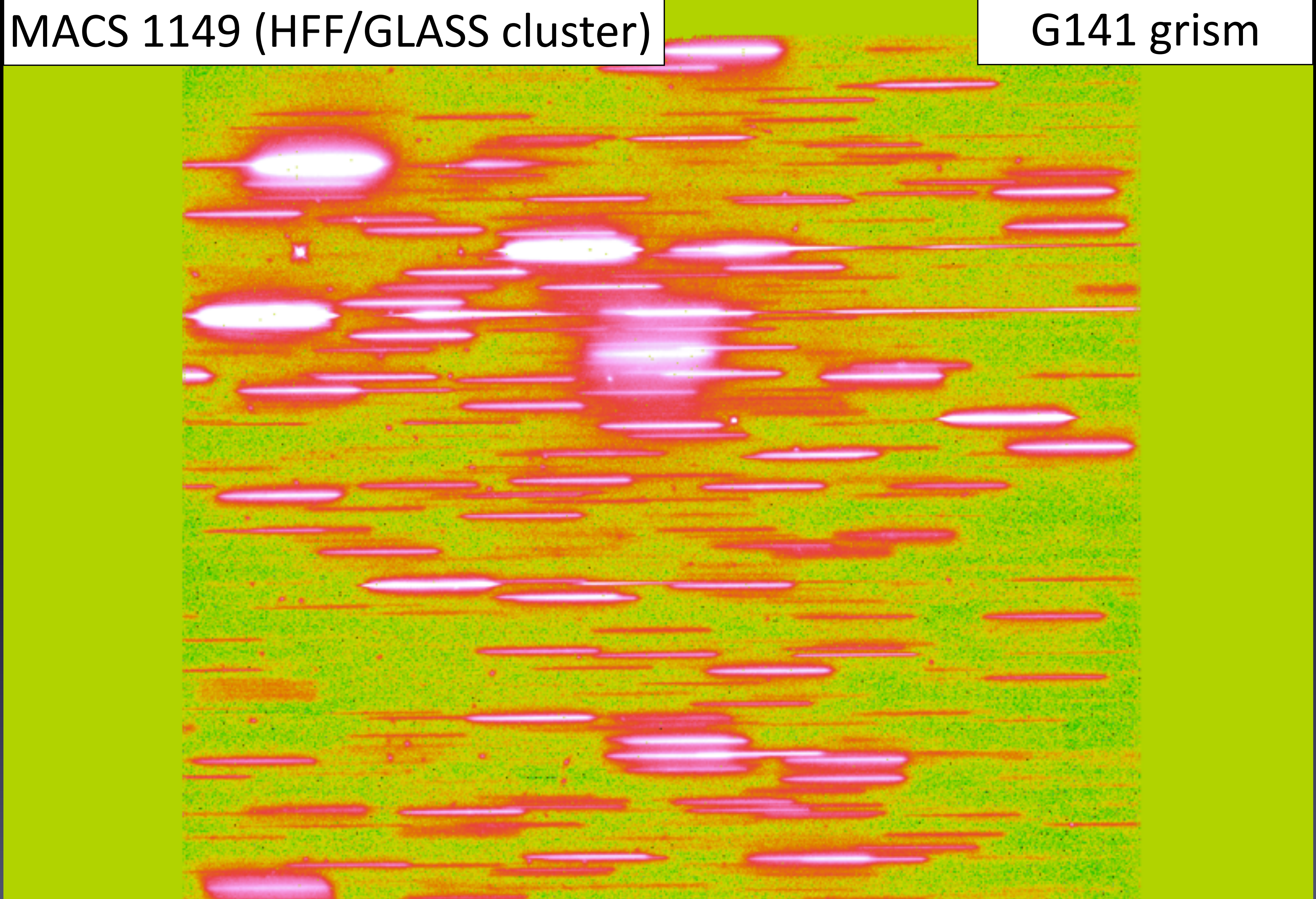

Wang et al. (2017) arXiv:1610.07558
Wang et al. (2019) arXiv:1808.08800
Wang et al. (2020) arXiv:1911.09841

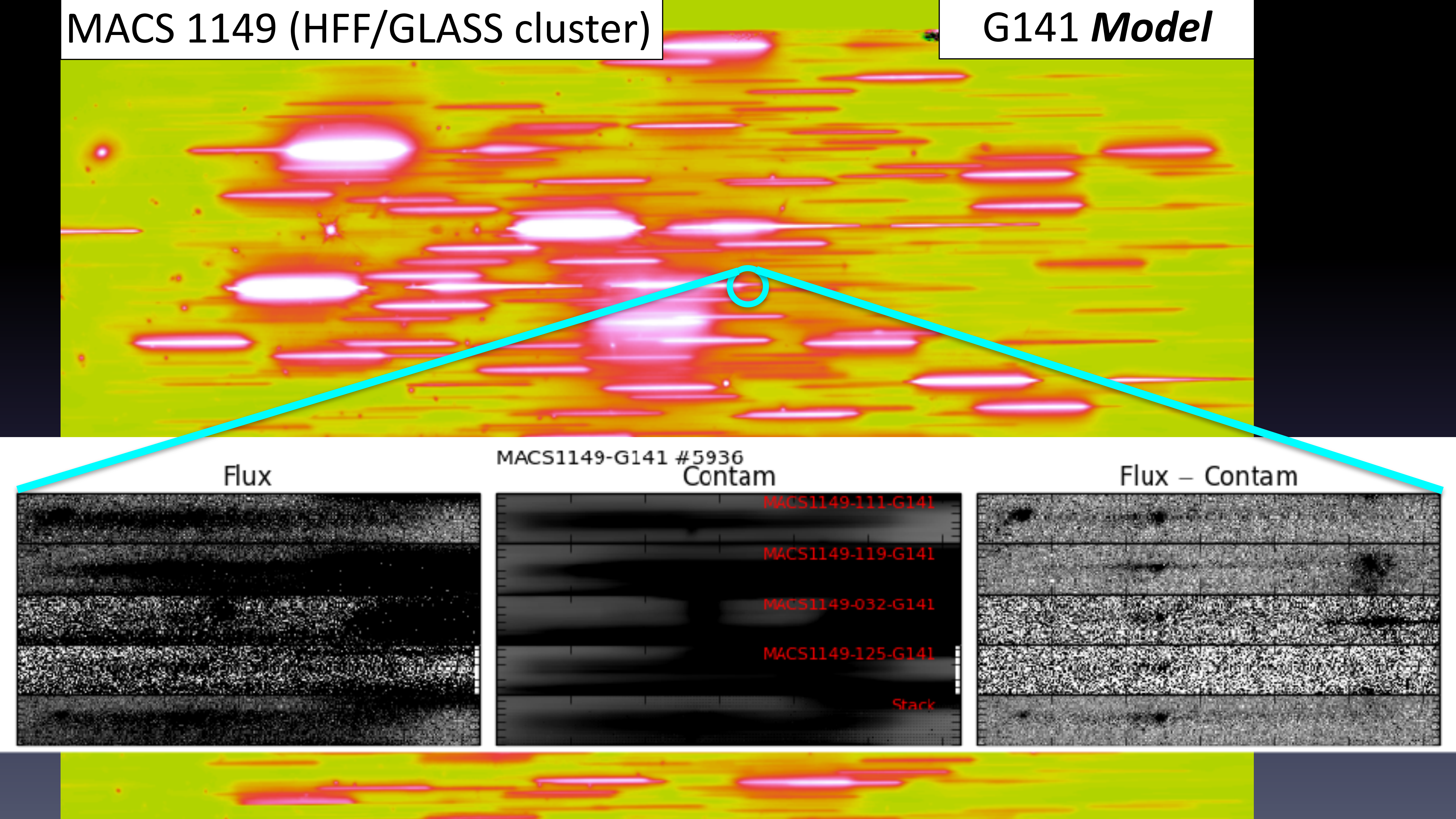
MACS 1149 (HFF/GLASS cluster)
G141 Model
MACS1149-G141 #5936
Flux
Contam
Flux – Contam
MACS1149-111-G141
MACS1149-119-G141
MACS1149-032-G141
MACS1149-125-G141
Stack

The forward-modeling extraction of grism data products

color-composite image

dispersed grism exposure

forward-modeled residual

Kelly et al. (2015), Wang et al. (2017)

Precise Mapping of Resolved Chemical Properties in High-z Galaxies

Data analysis for the Grism Lens-Amplified Survey from Space (GLASS) large HST program, HST-GO-13459, PI: Treu

140 HST orbits of G102 & G141

GLASS

in fields of 10 galaxy cluster centers

two dispersion directions

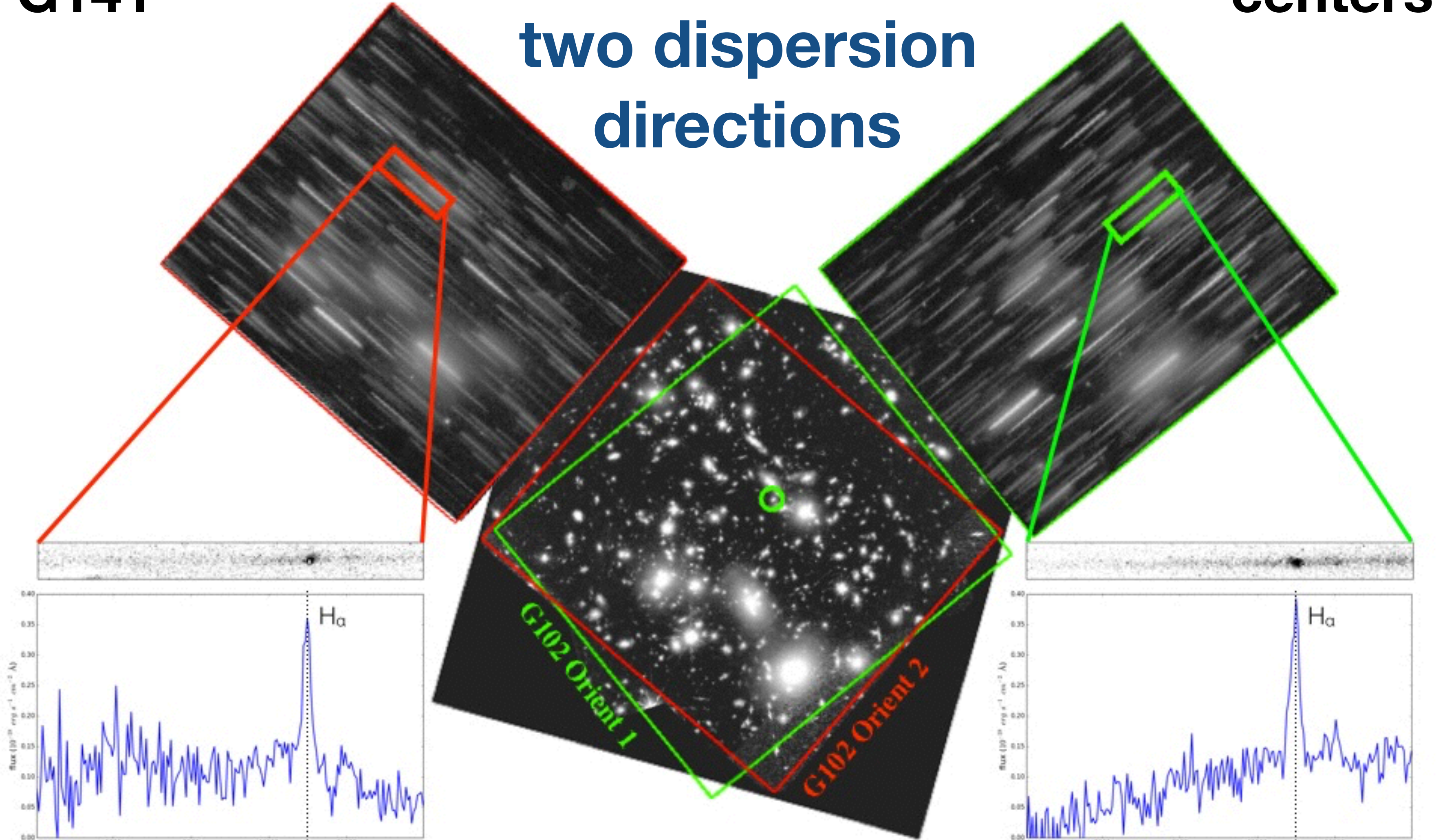

Schmidt et al. (2014), Treu et al. (2015)

The MAMMOTH-Grism Program

A unique sample of three most massive protoclusters at $z>2$ with diversity of the overdense environments

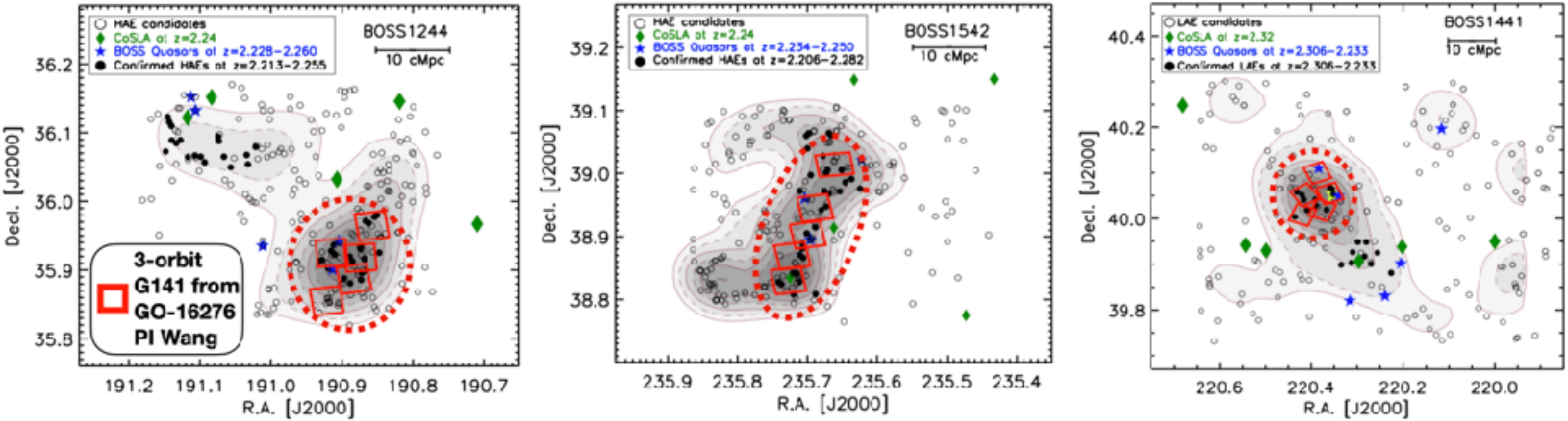

- MAMMOTH-Grism (HST-GO-16276, **PI: Wang**) is a Cycle-28 HST medium GO program awarded 45 orbits of WFC3/G141 spectroscopy, targeting the density peak regions of the three most massive galaxy proto-clusters at z ~ 2 − 3. Co-Is: Prof. **Zheng Cai** and **Zihao Li**

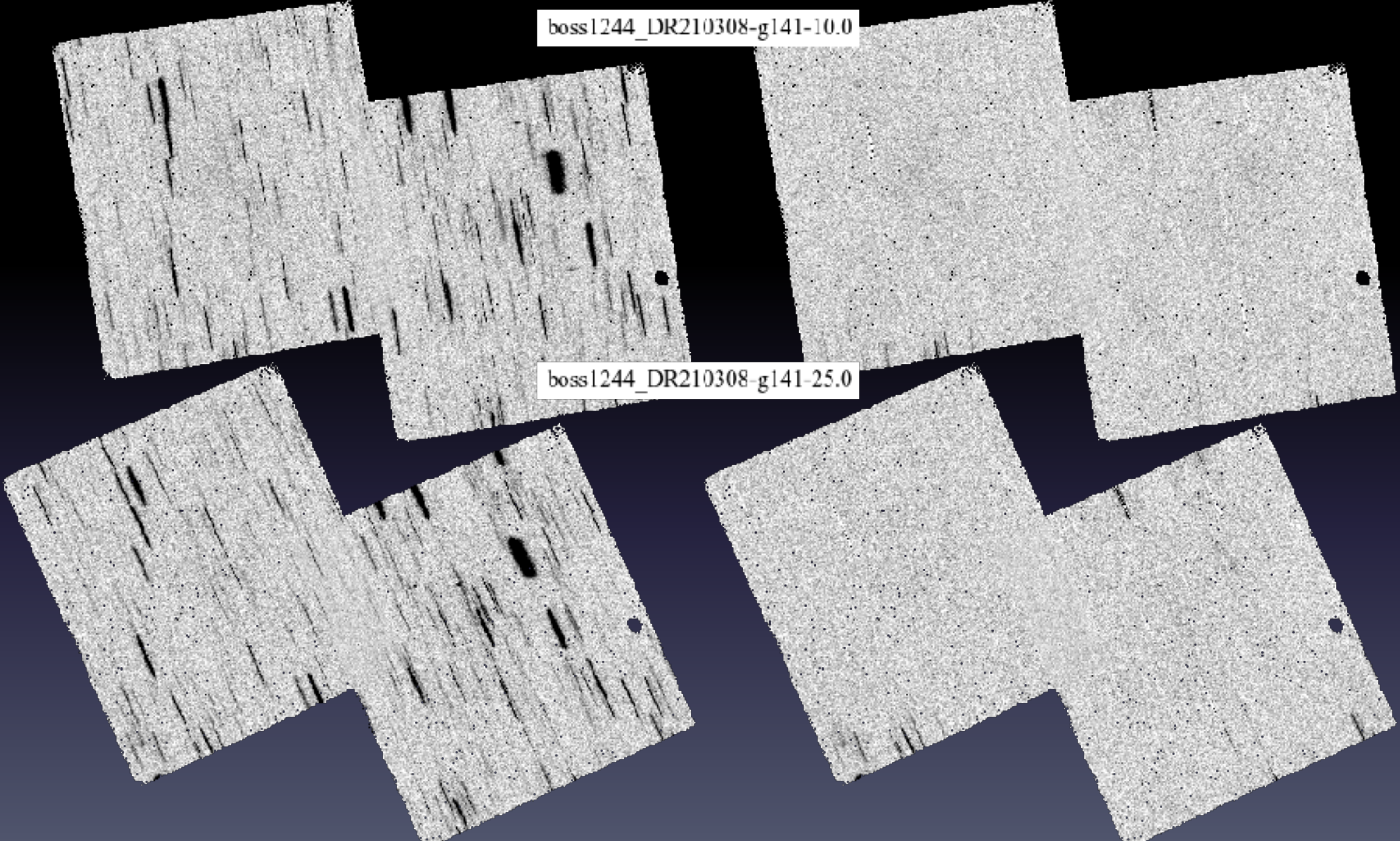
boss1244_DR210308-g141-10.0
boss1244_DR210308-g141-25.0

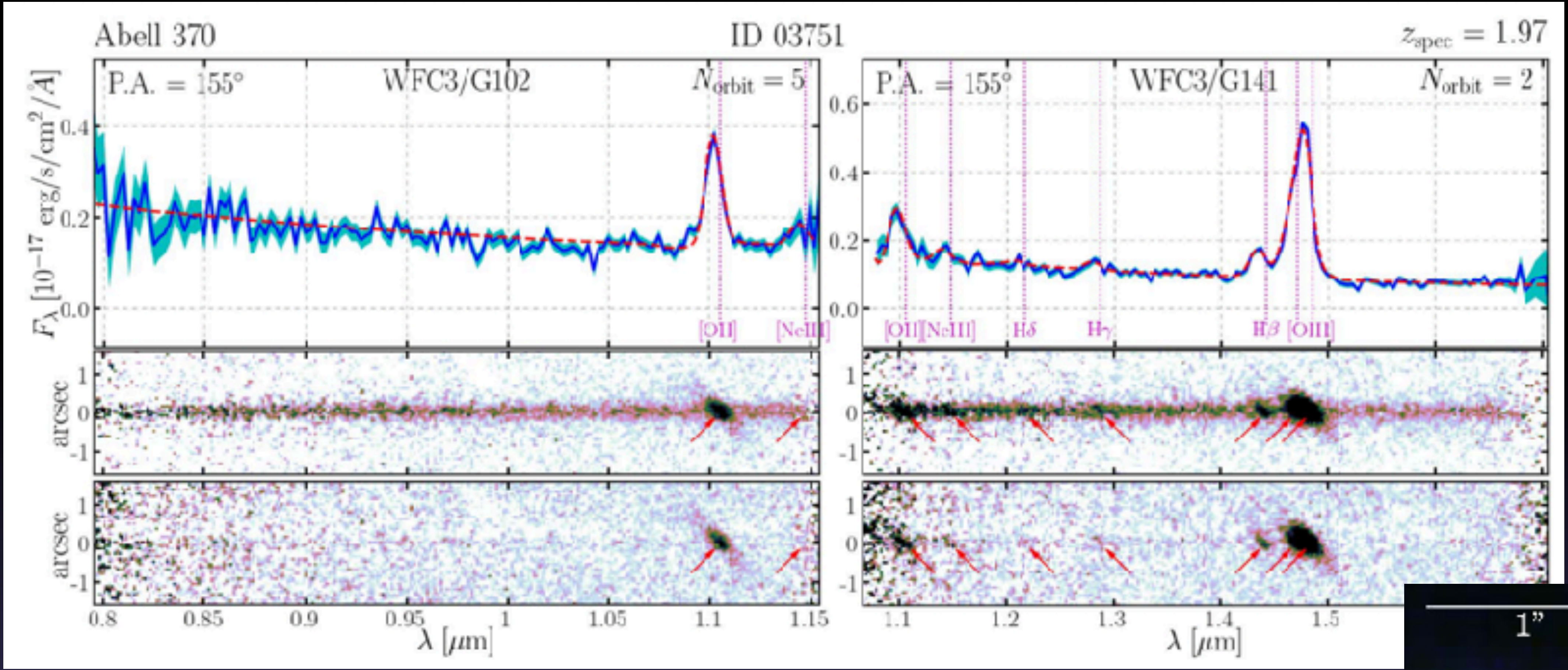

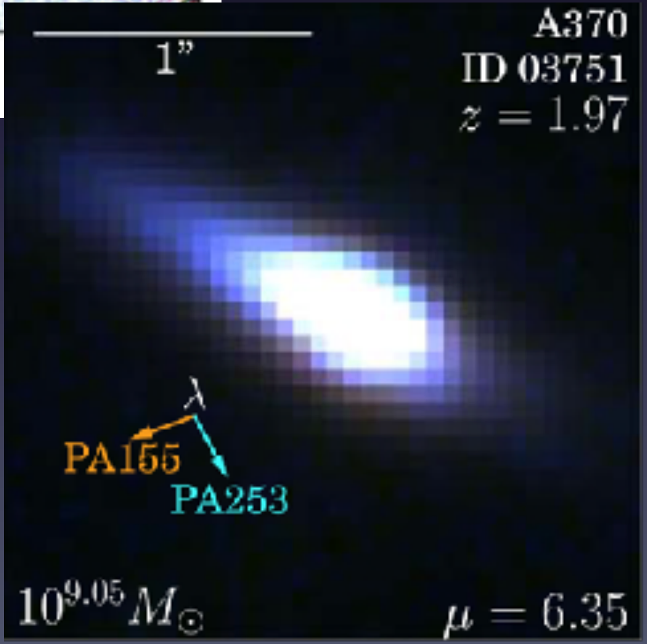

The 1D/2D grism spectra extracted for a z~2 dwarf galaxy (Mstar ~ 1e9 Msun).

- **blue** solid: optimally extracted 1D spectra
- **cyan** band: 1-sigma uncertainty
- **red** dashed: forward modeled 1D spectra

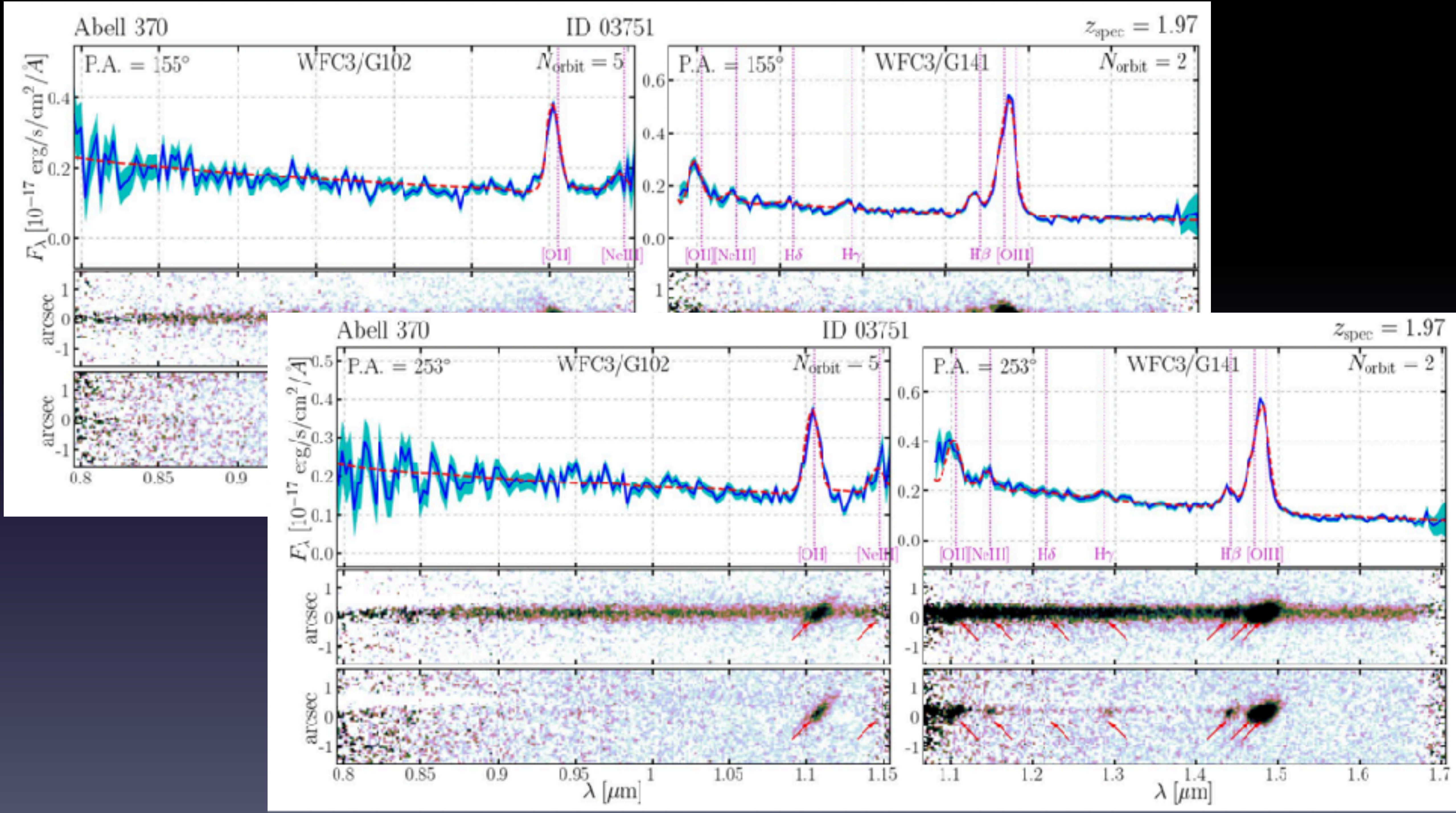
Abell 370
ID 03751
$z_{\rm spec} = 1.97$
P.A. = 155°
WFC3/G102
$N_{\rm orbit} = 5$
WFC3/G141
$N_{\rm orbit} = 2$
P.A. = 253°
F_λ [10^{-17} erg/s/cm^2/Å]
arcsec
[OII]
[NeIII]
Hδ
Hγ
Hβ
[OIII]
λ [μm]

Deblending neighboring emission lines of same source

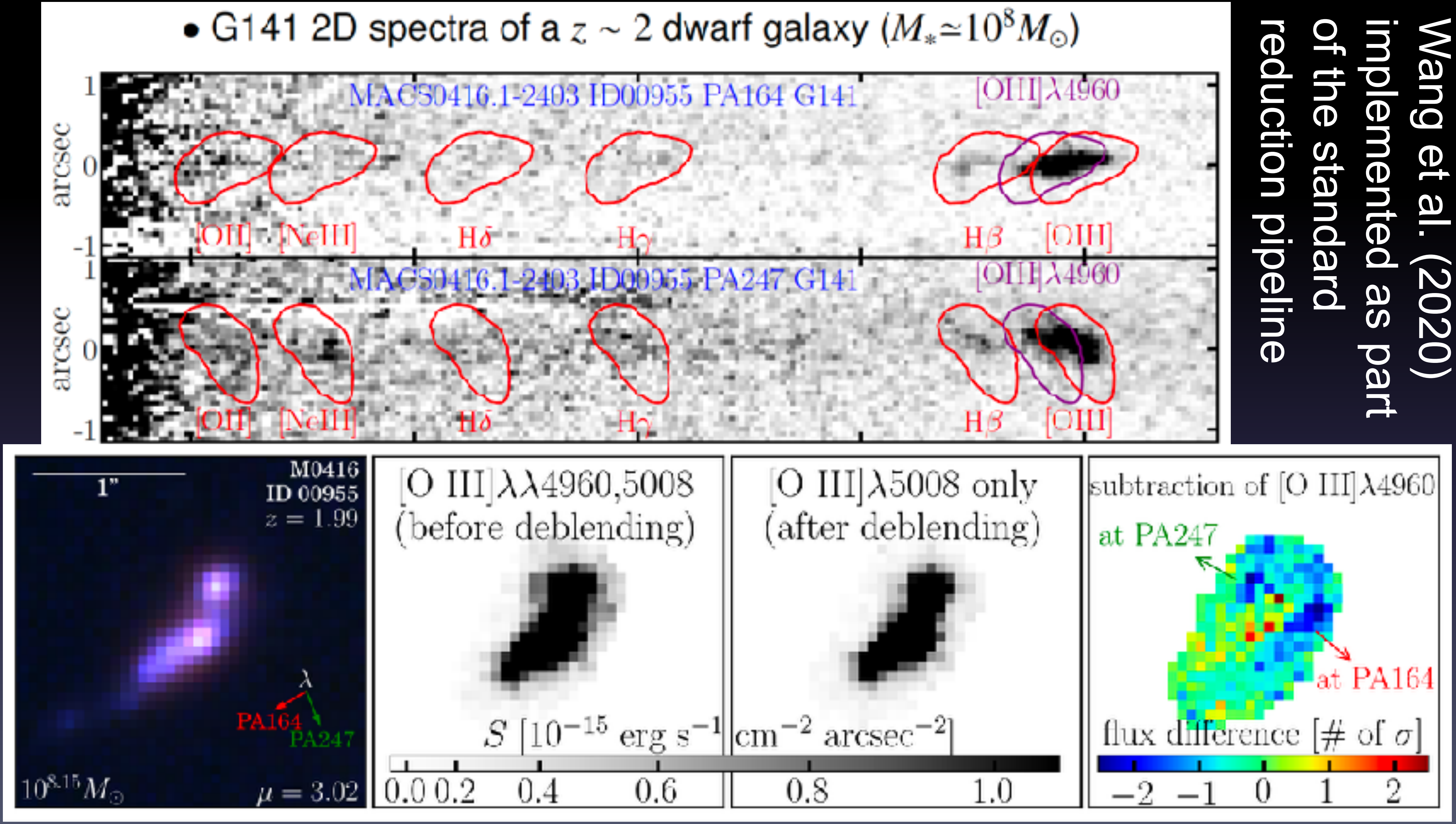

Wang et al. (2020) implemented as part of the standard reduction pipeline

2D emission line maps from grism data: turning the grism instrument into an IFU!

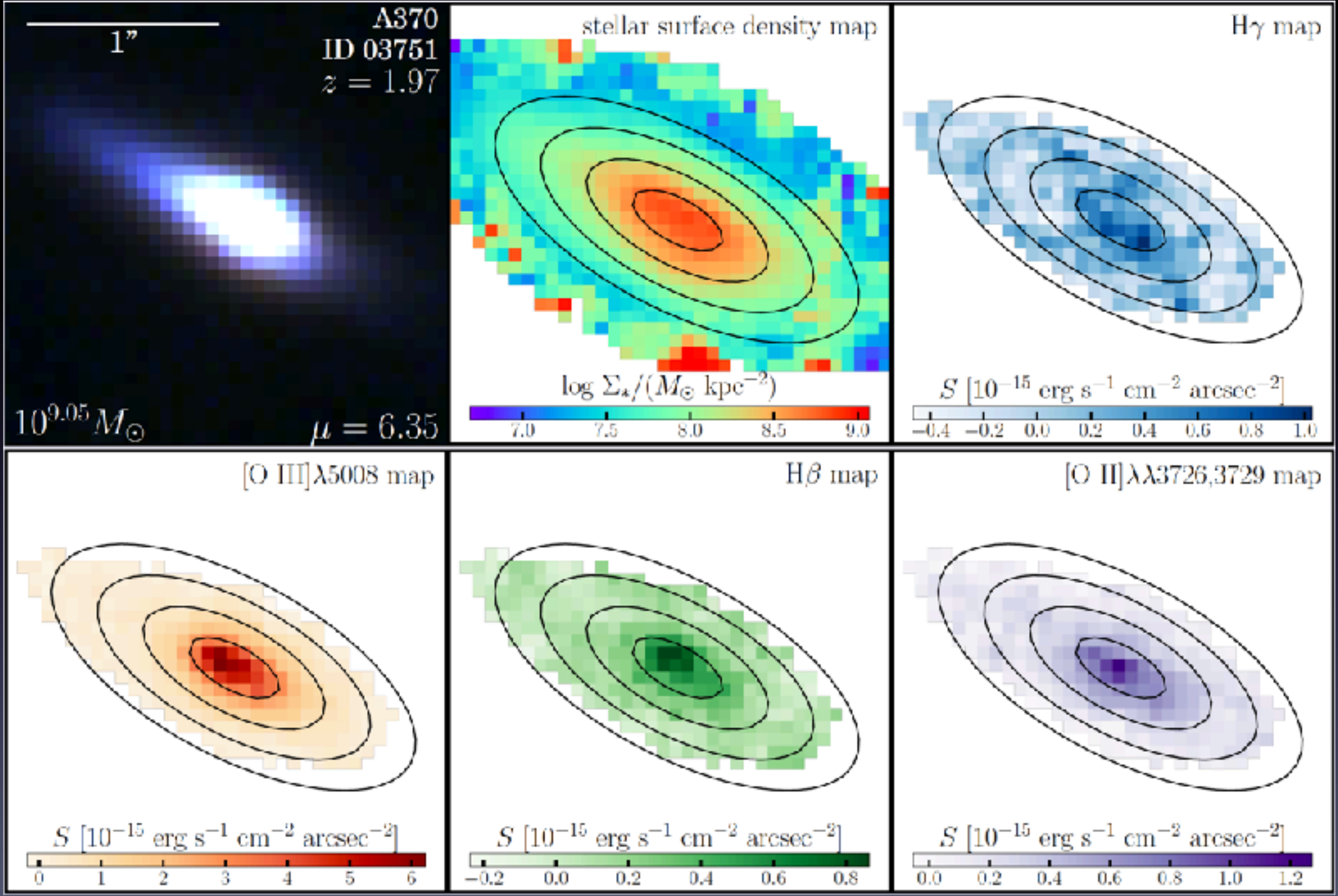

A novel Bayesian forward-modeling diagnostic method

a stack of Keck mosfire spectra

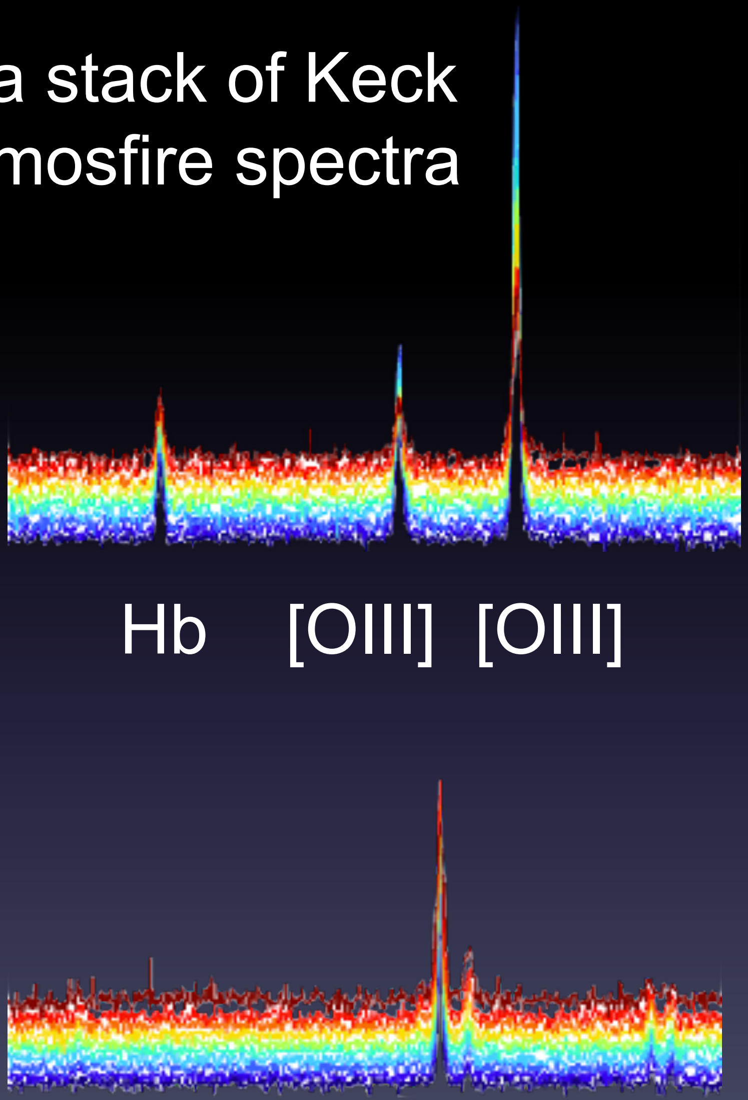

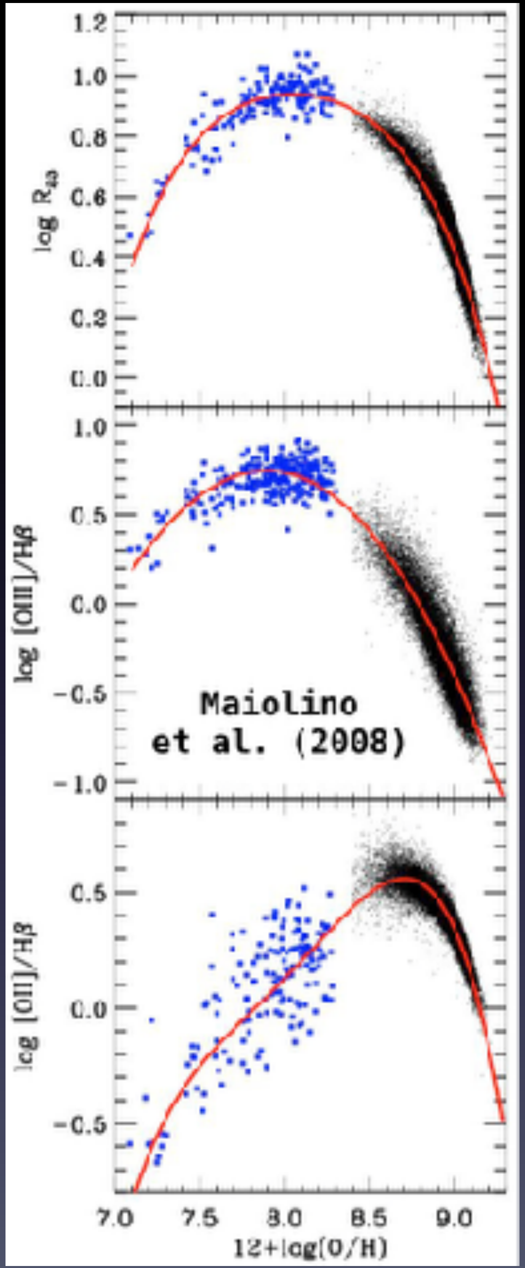

- metallicity
- ionization
- excitation
- electron density
- ISM temperature
- etc.

A novel Bayesian forward-modeling diagnostic method

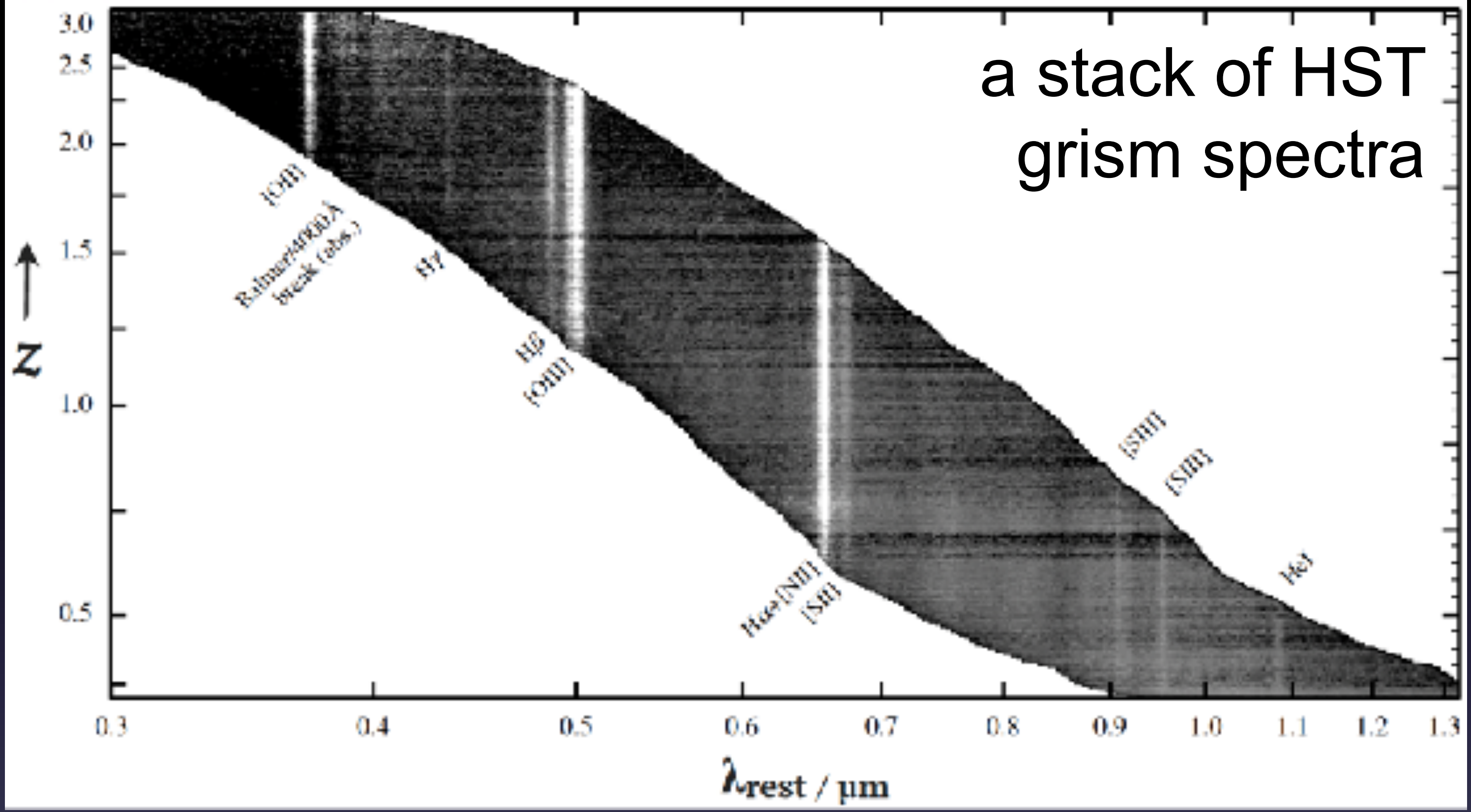

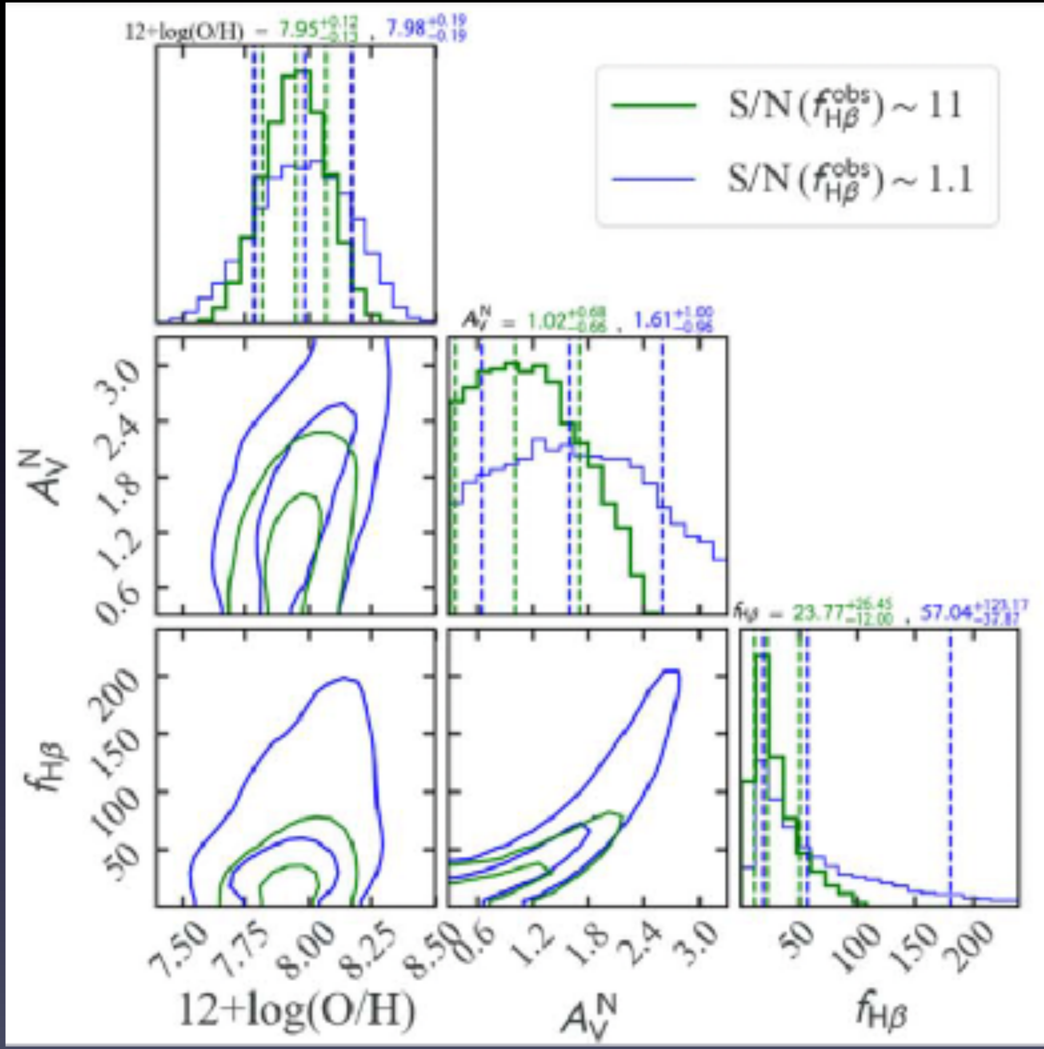

forward-model line fluxes directly:

$$\chi^2 = \sum_i \frac{\left(f_{\mathrm{EL}_i} - R_i \cdot f_{\mathrm{H}\beta}\right)^2}{(\sigma_{\mathrm{EL}_i})^2 + \left(f_{\mathrm{H}\beta}\right)^2 \cdot (\sigma_{R_i})^2}$$

Discovery of strongly inverted metal gradients at high z

- analytical chemical evolution model of galaxy formation assuming inside-out growth predicts initially steep negative gradients flatten over time

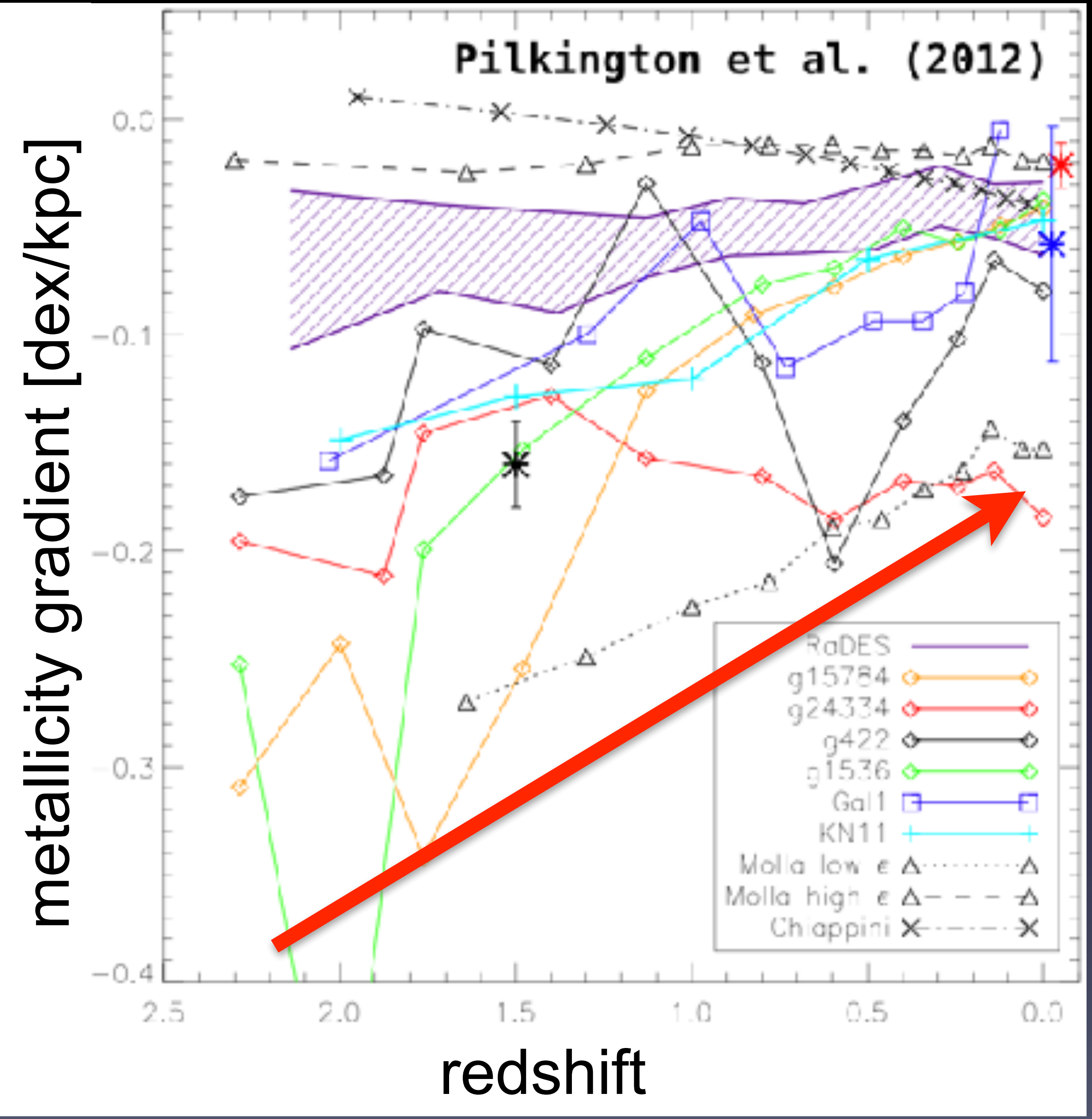

Discovery of strongly inverted metal gradients at high z

- analytical chemical evolution model of galaxy formation assuming inside-out growth predicts initially steep negative gradients flatten over time
- cosmological hydrodynamic simulations instead predict that metallicities are initially well mixed by strong feedback and later locked into a negative slope

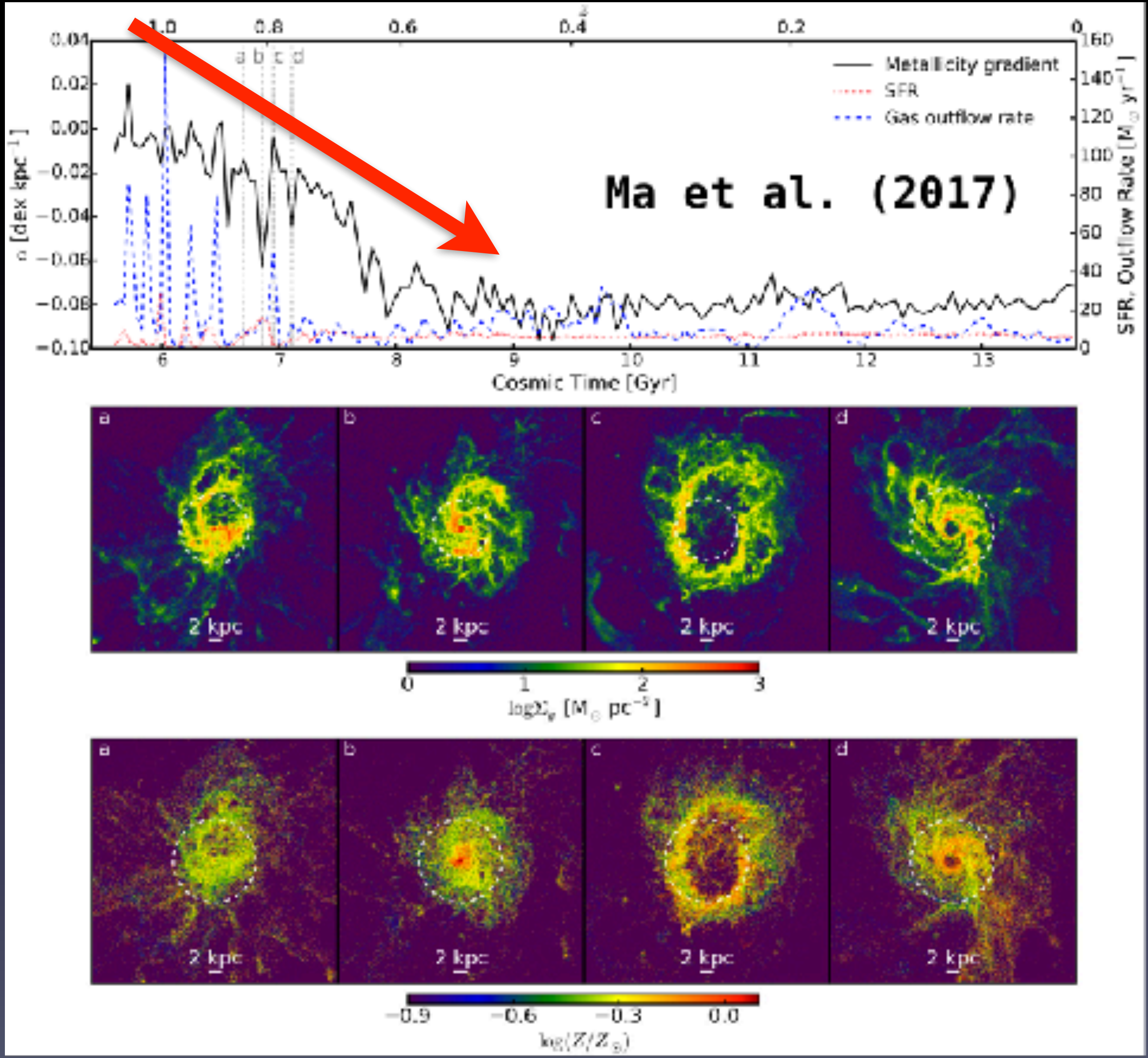

Discovery of strongly inverted metal gradients at high z

- analytical chemical evolution model of galaxy formation assuming inside-out growth predicts initially steep negative gradients flatten over time
- cosmological hydrodynamic simulations instead predict that metallicities are initially well mixed by strong feedback and later locked into a negative slope
- we obtained the first measurements with sub-kpc spatial resolution of strongly inverted (i.e. positive) metal gradients in dwarf galaxies

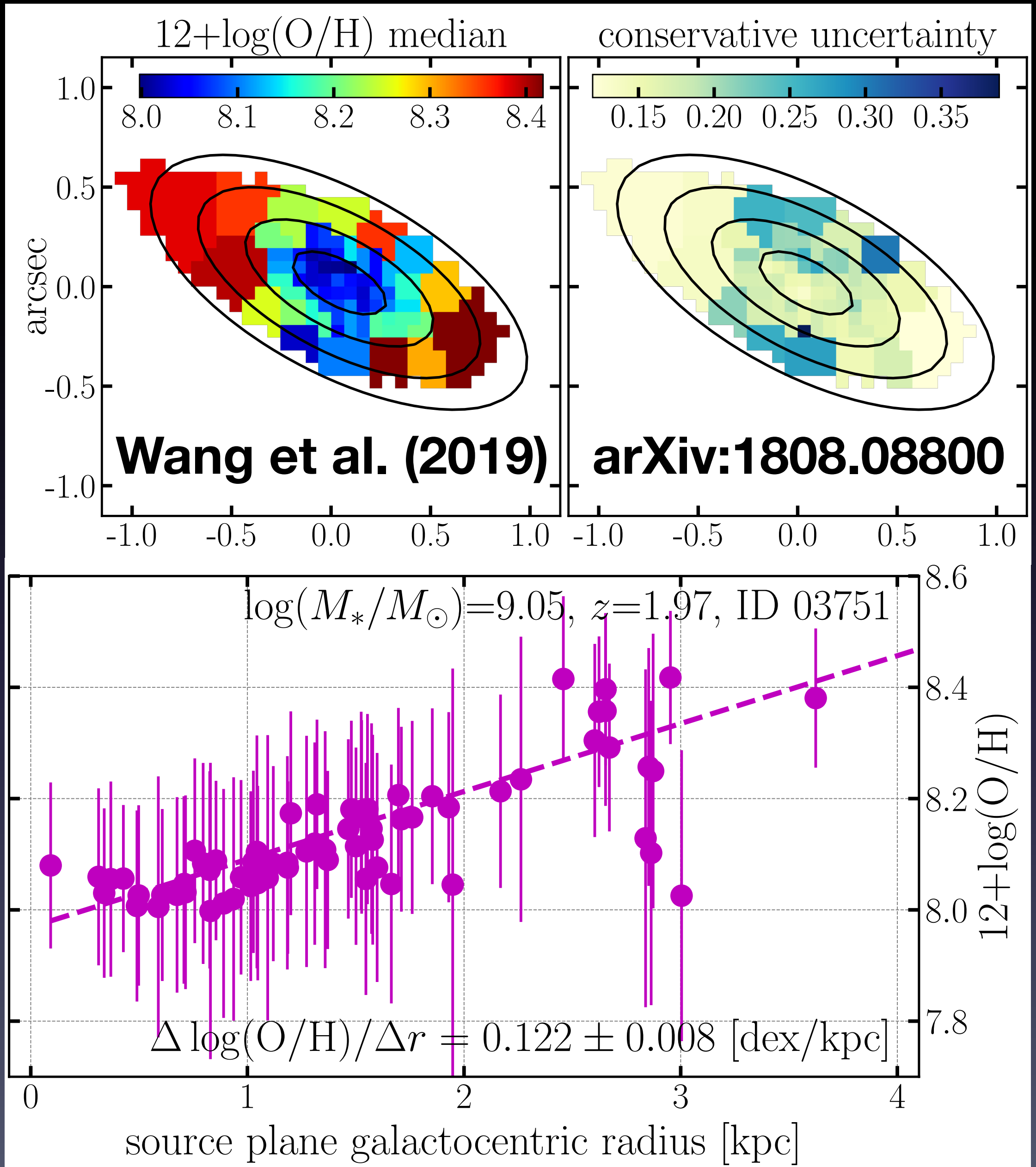

The reasons for galaxies showing inverted gradients

1. metal-enriched gas outflows triggered by powerful galactic winds that transport metals from galaxy center to outskirts

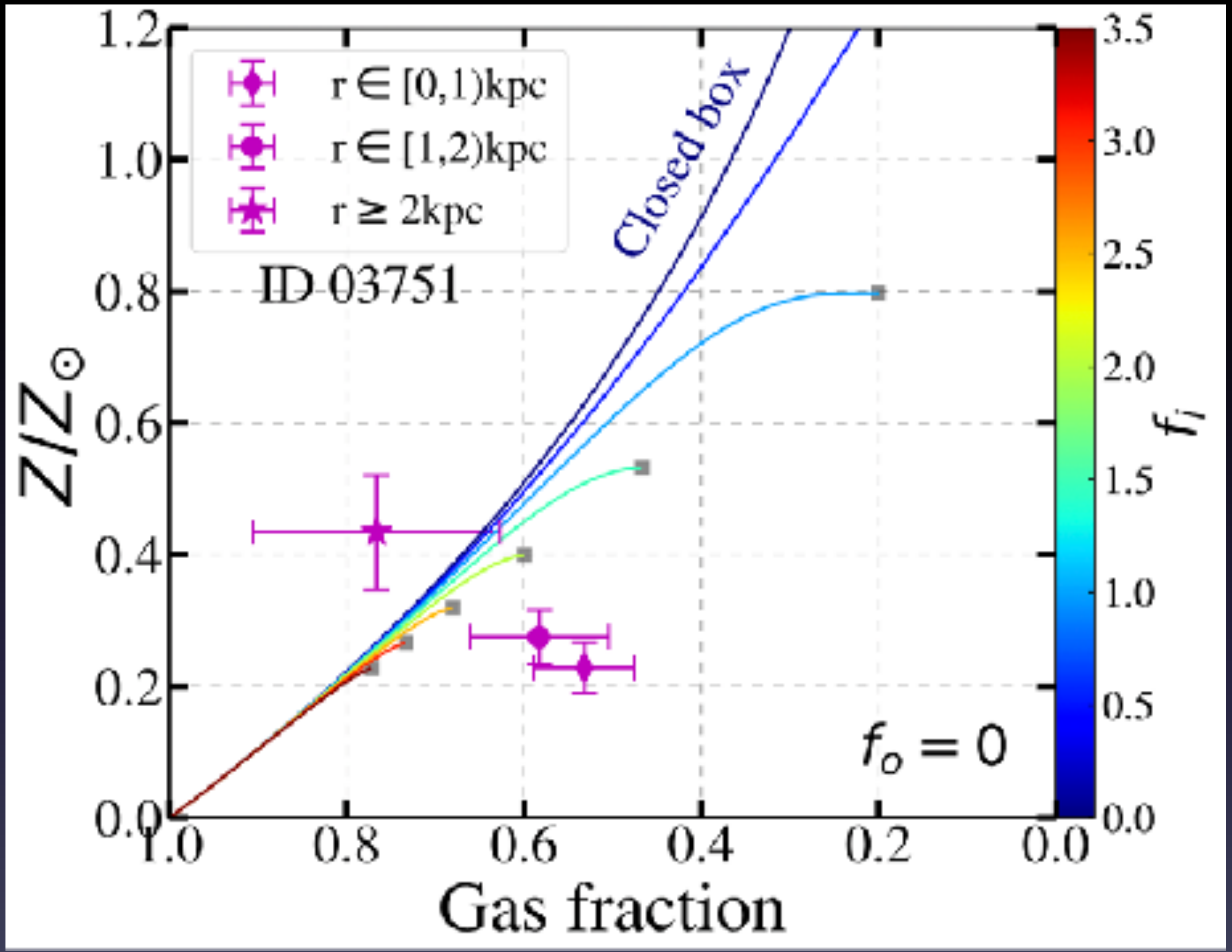

gas inflows alone cannot explain

The reasons for galaxies showing inverted gradients

1. metal-enriched gas outflows triggered by powerful galactic winds that transport metals from galaxy center to outskirts

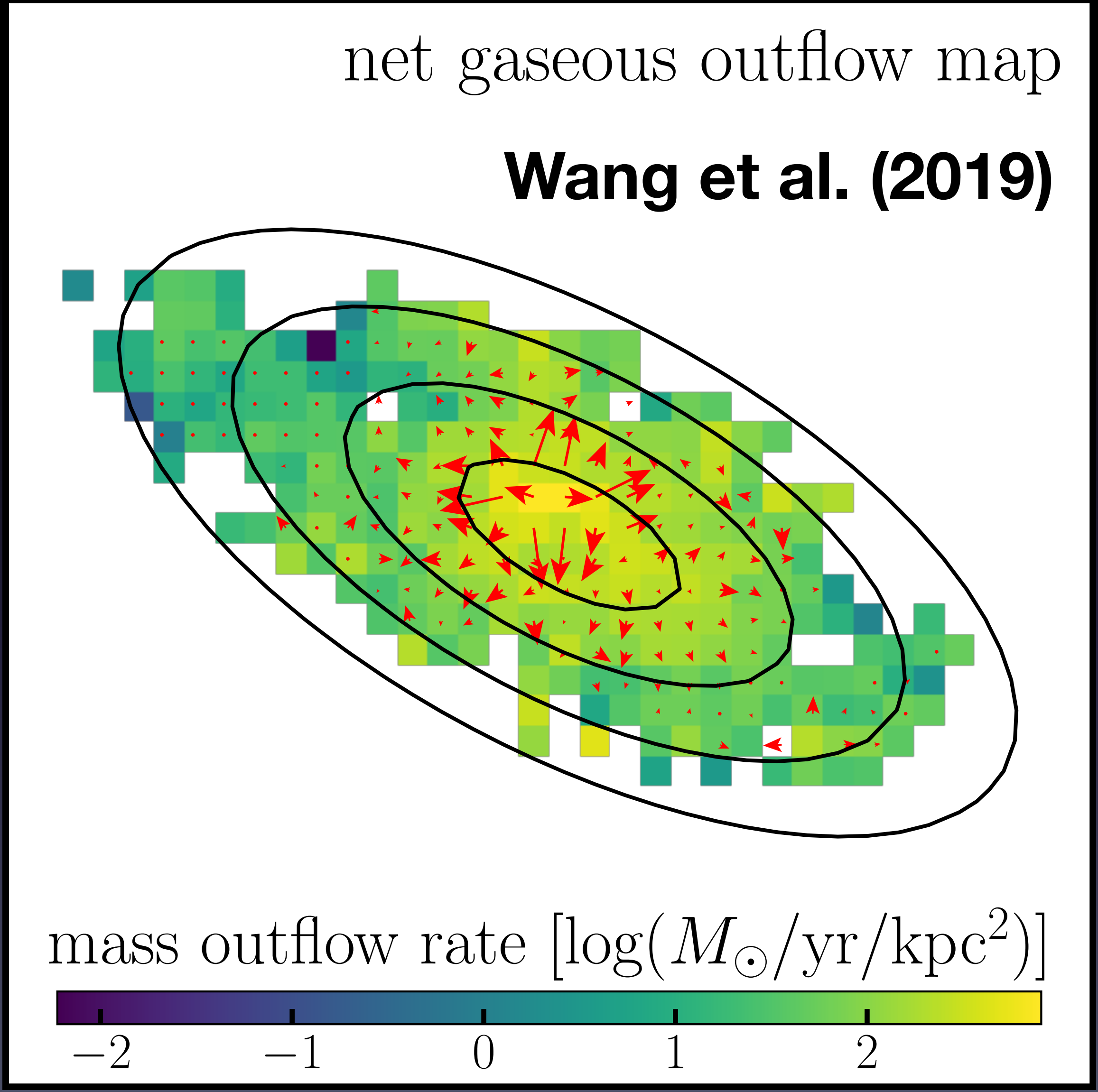

The reasons for galaxies showing inverted gradients

1. metal-enriched gas outflows triggered by powerful galactic winds that transport metals from galaxy center to outskirts
2. centrally-directed cold-mode gas accretion driven by the massive dark matter halos underlying galaxy protoclusters

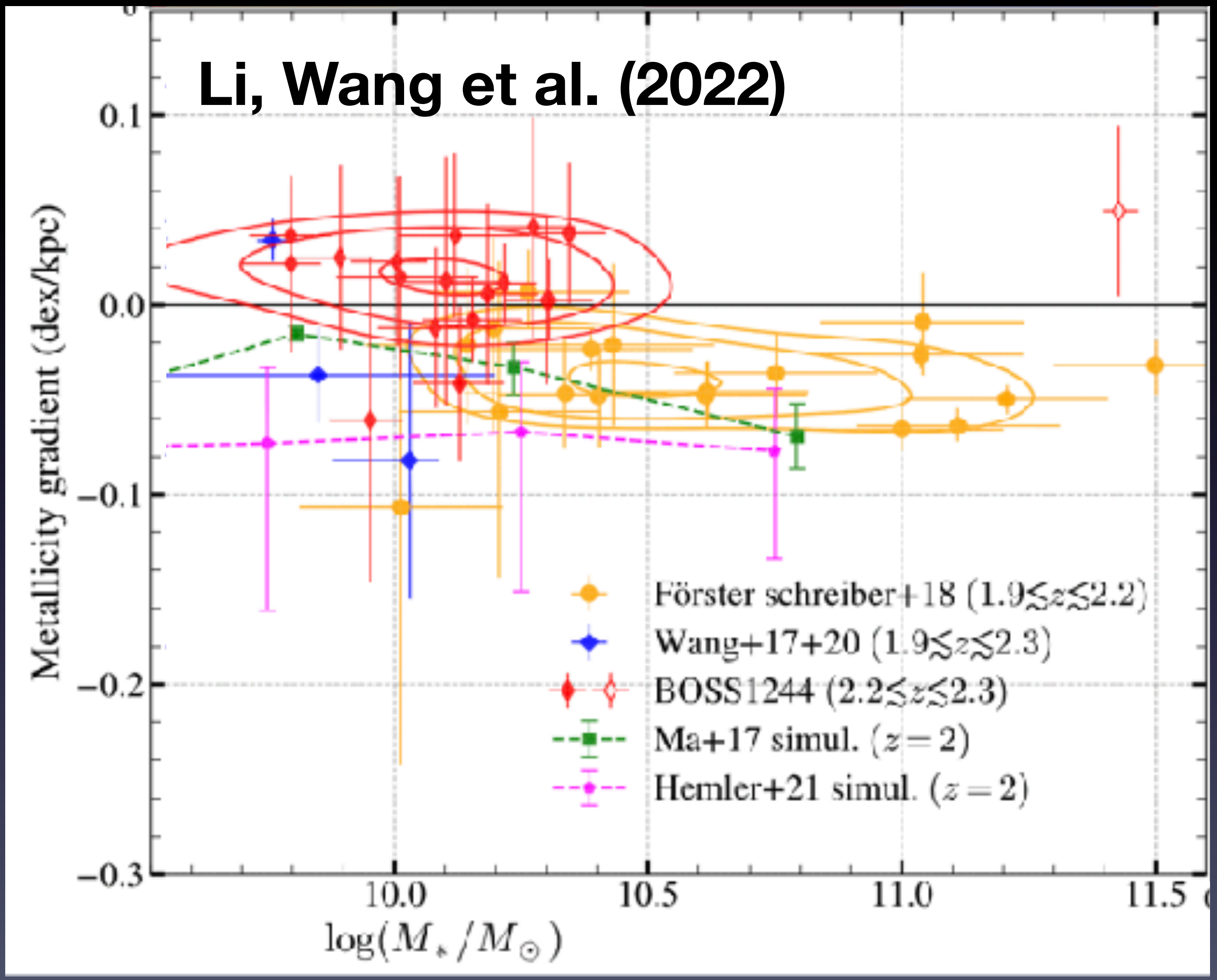

The reasons for galaxies showing inverted gradients

1. metal-enriched gas outflows triggered by powerful galactic winds that transport metals from galaxy center to outskirts
2. centrally-directed cold-mode gas accretion driven by the massive dark matter halos underlying galaxy protoclusters

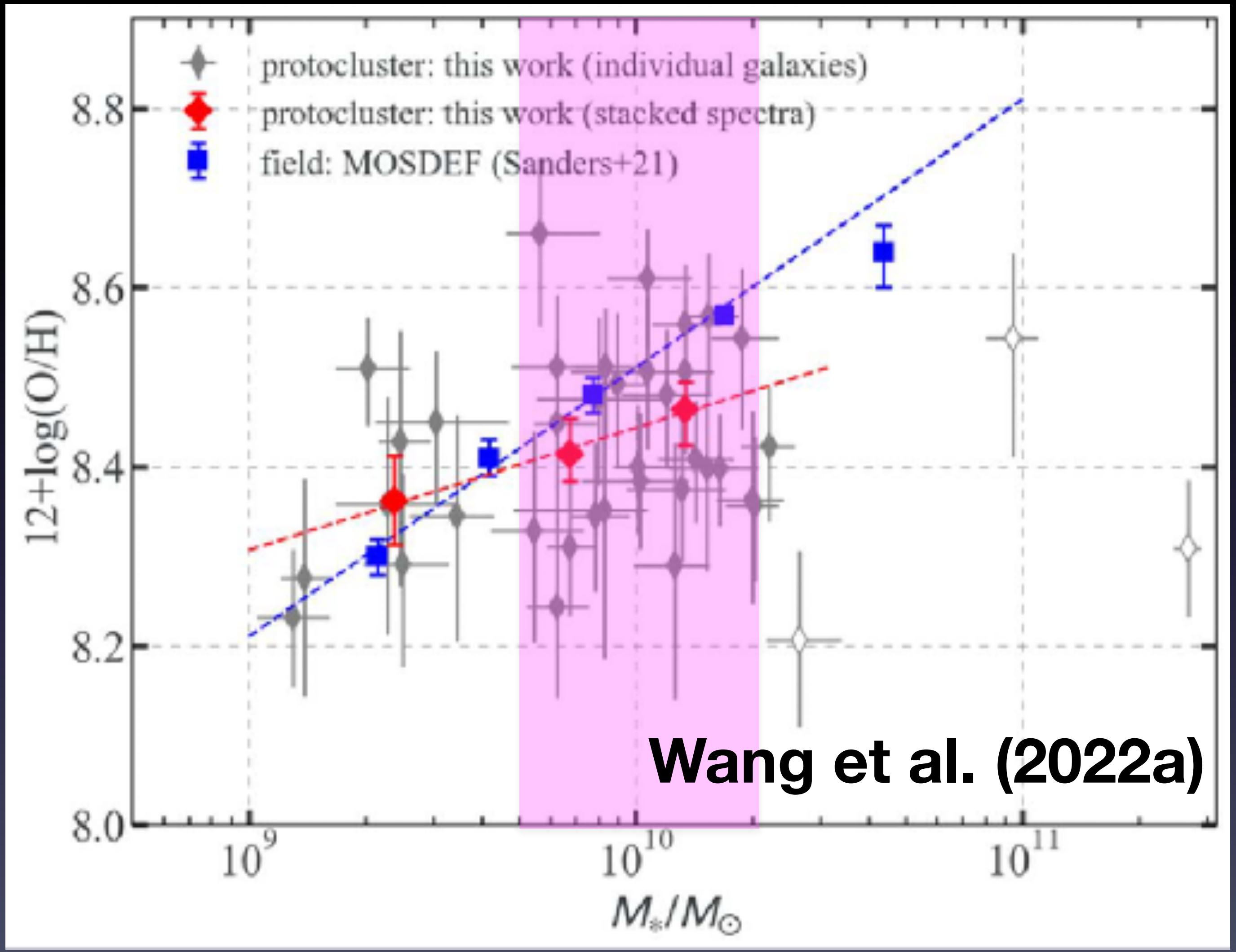

Wang et al. (2022a)

The reasons for galaxies showing inverted gradients

1. metal-enriched gas outflows triggered by powerful galactic winds that transport metals from galaxy center to outskirts
2. centrally-directed cold-mode gas accretion driven by the massive dark matter halos underlying galaxy protoclusters
3. metal-poor gas inflows to the inner galaxy disks induced by the strong tidal torques of close gravitational interactions

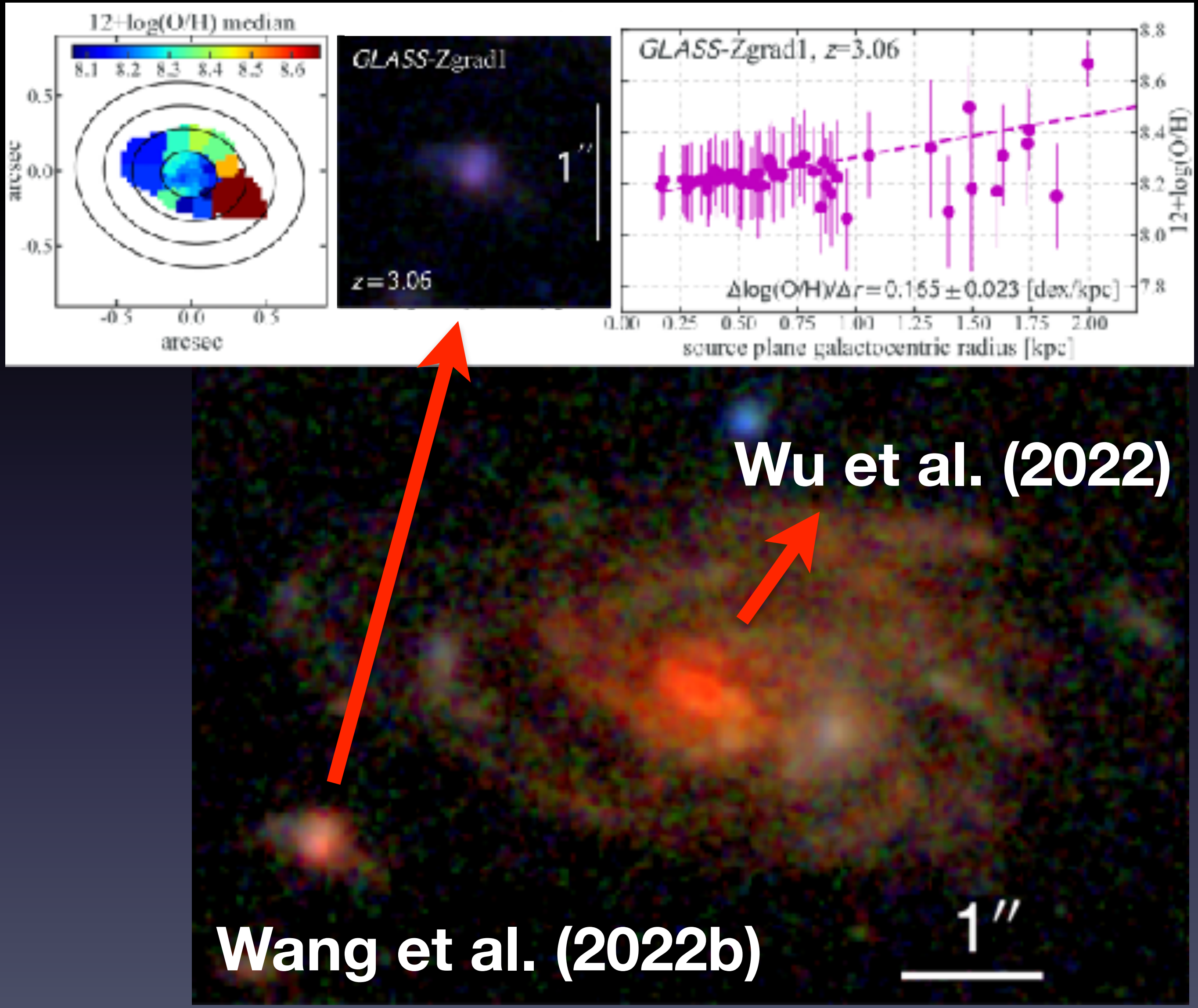

JWST/NIRISS Slitless Spectroscopy of Abell 2744

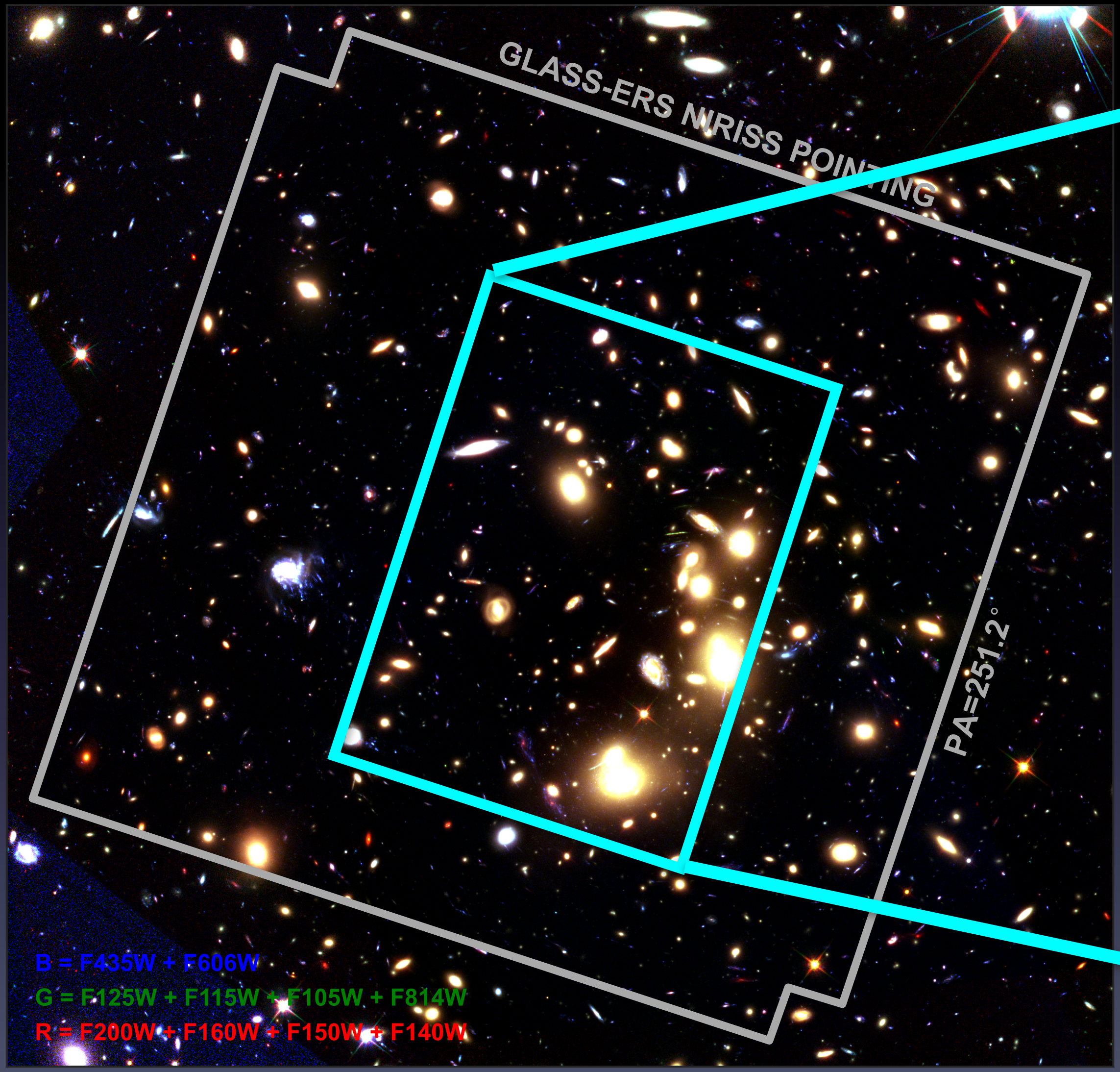

Based on JWST-ERS-1324, PI: Treu et al. (2022)

JWST/NIRISS Slitless Spectroscopy of Abell 2744

dispersion direction

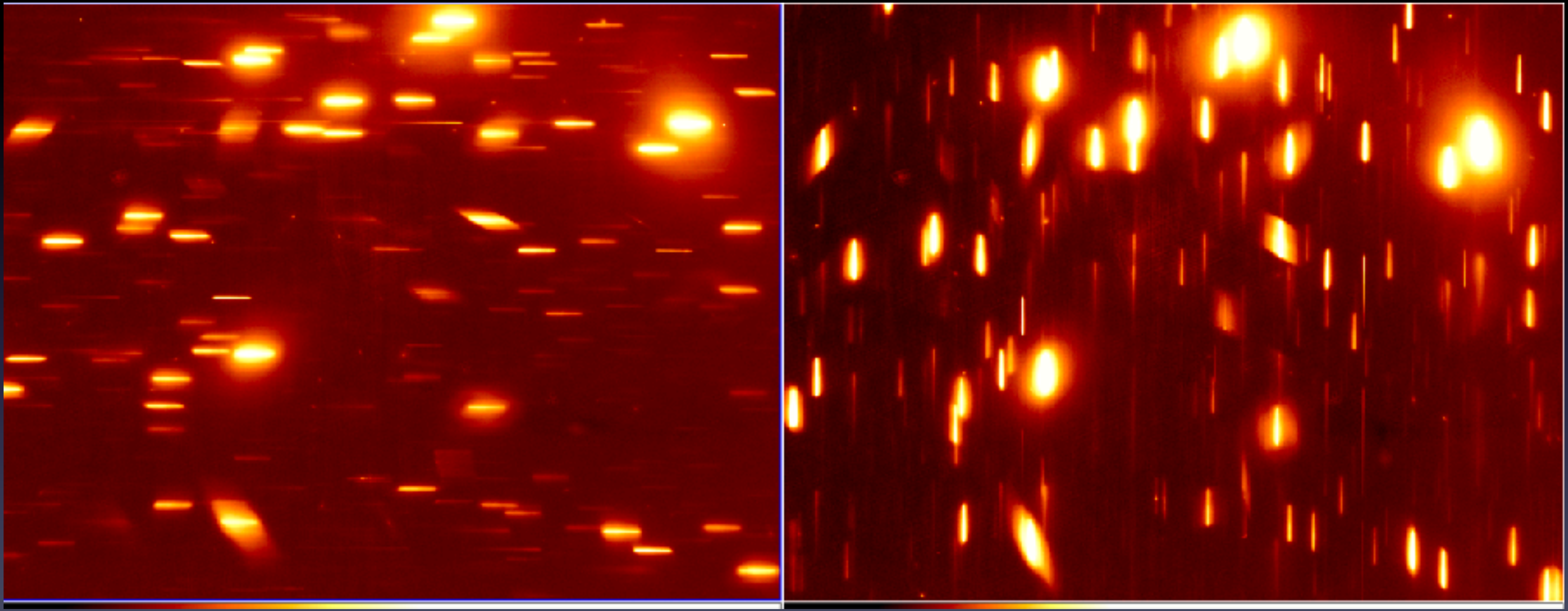

without rotating the telescope

The first spatially resolved analysis from JWST grisms

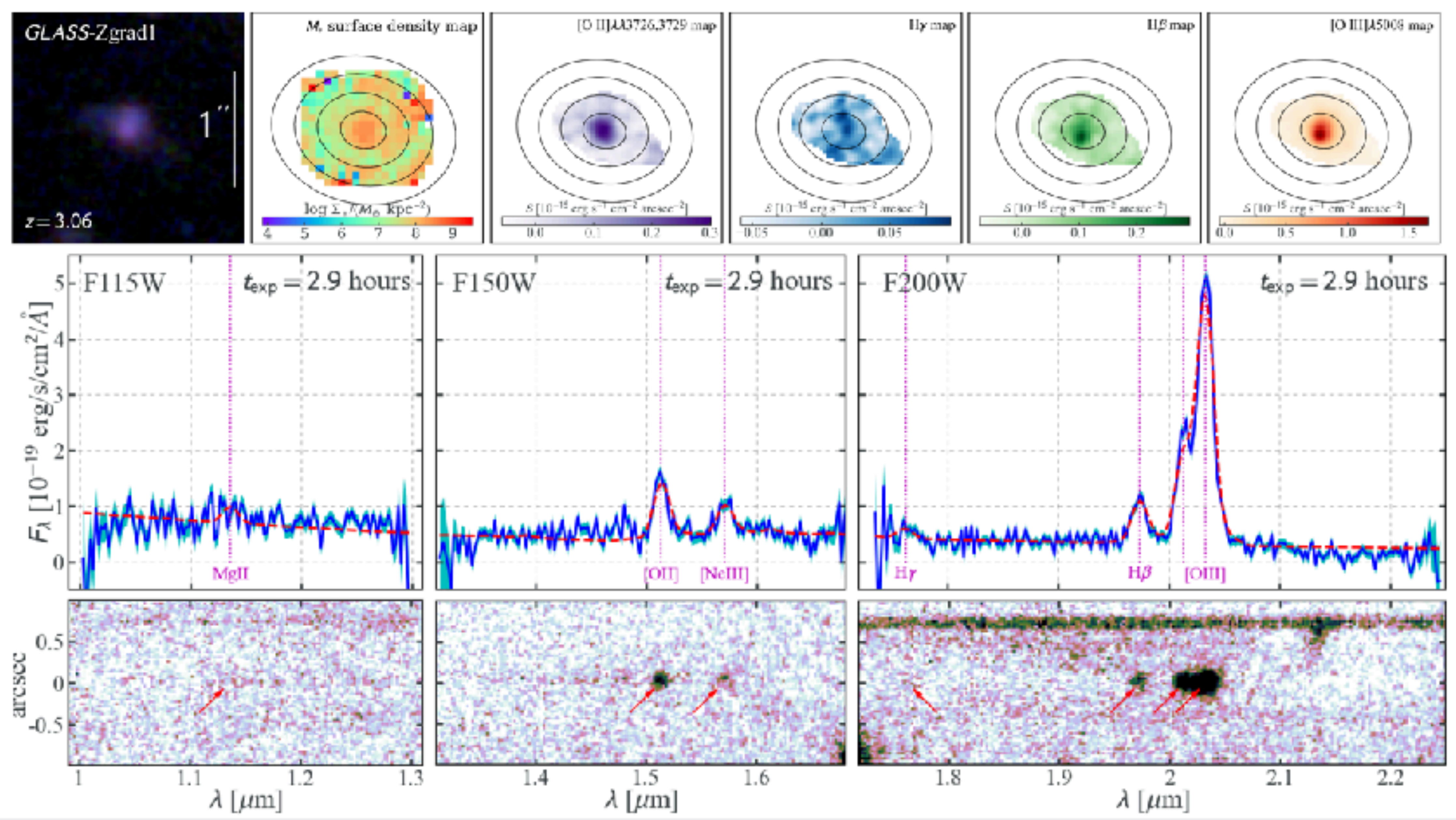

Wang et al. (2022b) arXiv:2207.13113

The first metal gradient with sub-kpc resolution at z≥3

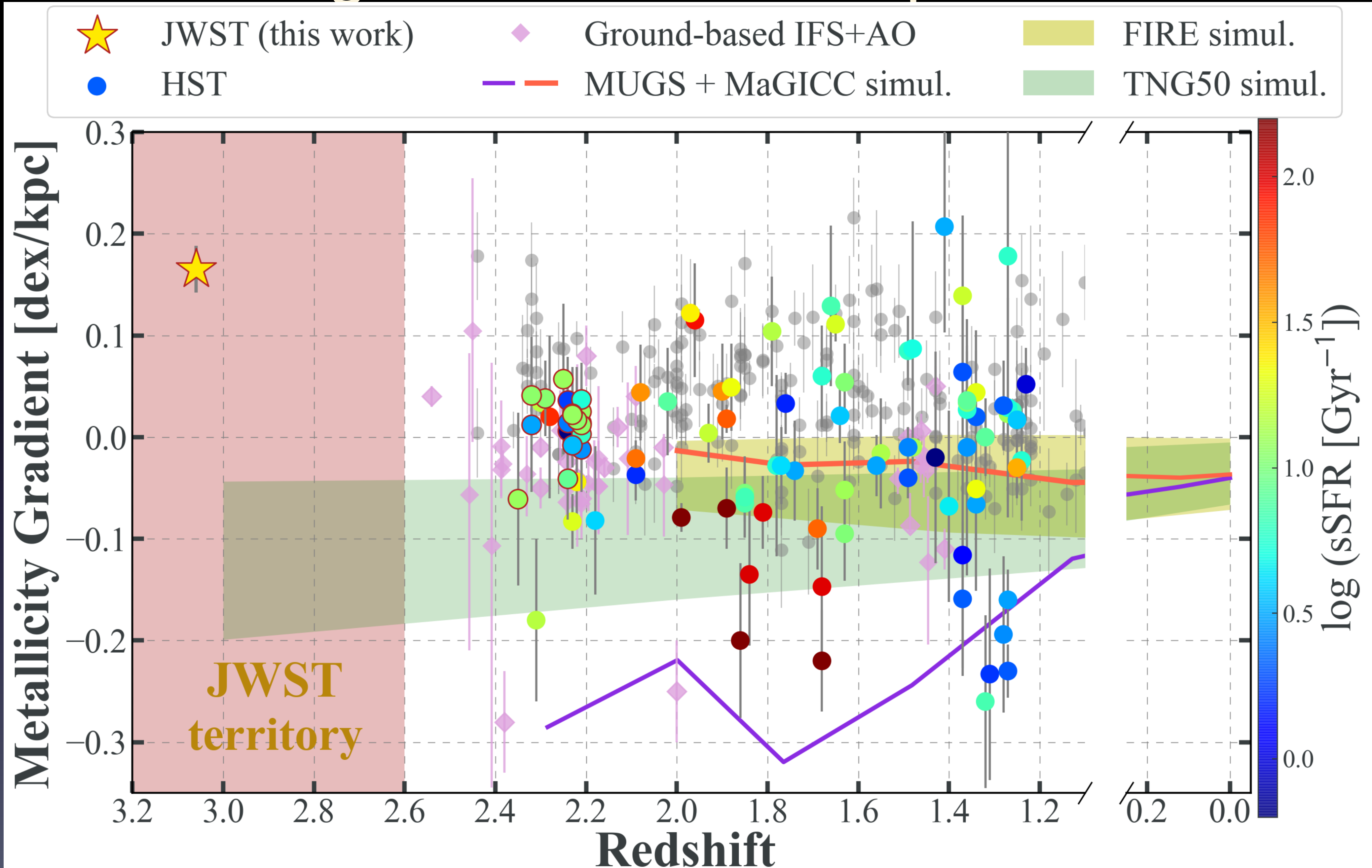

Wang et al. (2022b) arXiv:2207.13113

Part I: Space-based Wide-field Slitless Spectroscopy

Part II: Space-based Near-Ultraviolet Imaging

Part III: Prospect for our CSST Main Survey blue: UV + blue (new), green: mid-optical, red: near-infrared

The entire survey: ~140,000 galaxies

This picture (3'.9×2'.2): >5,000 galaxies blue: UV + blue (new), green: mid-optical, red: near-infrared

The entire survey: ~140,000 galaxies

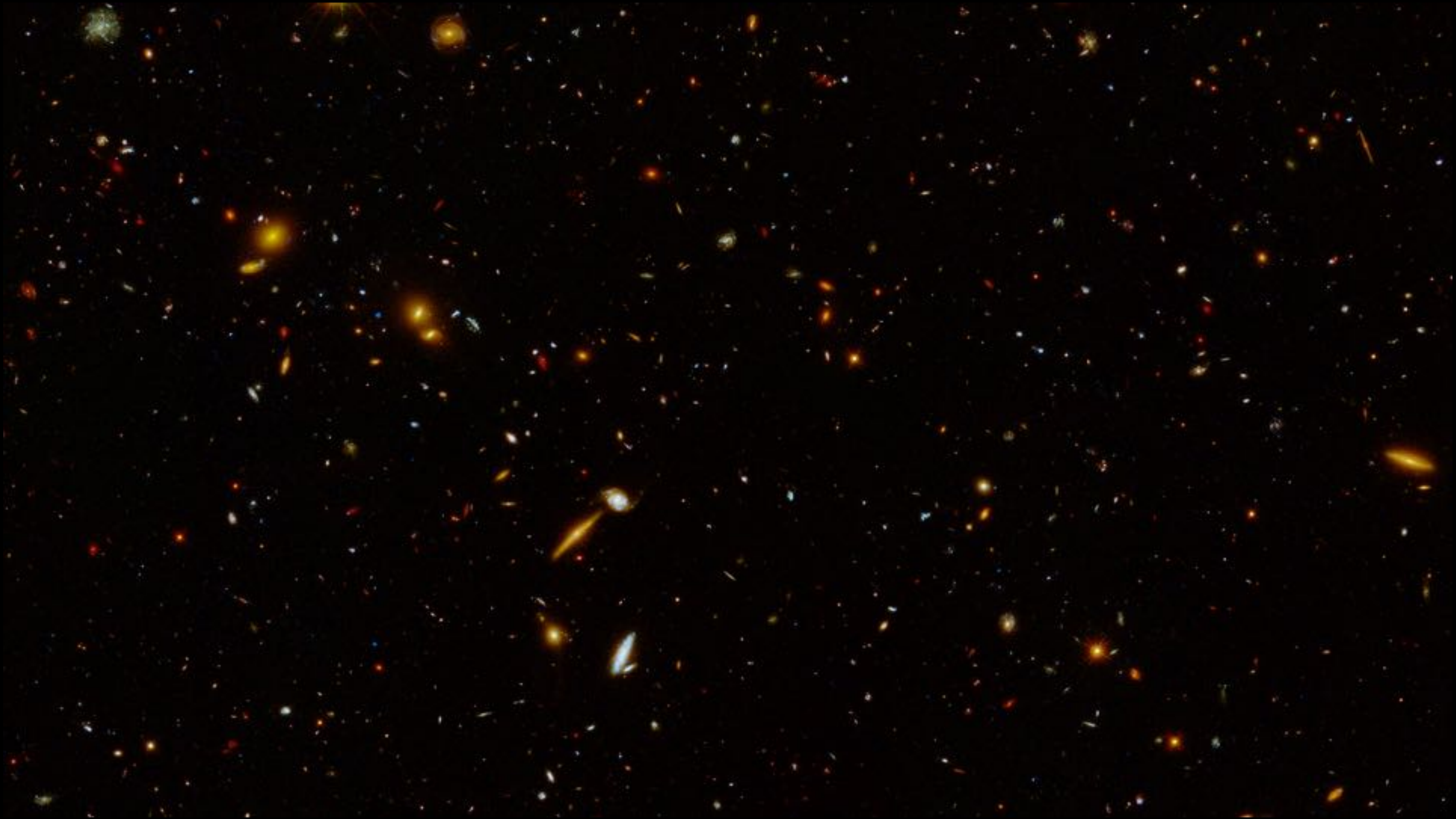

This picture (3’.9×2’.2): >5,000 galaxies

UVCANDELS: the UV imaging of the CANDELS fields

- CANDELS is *Hubble*'s largest survey of distant galaxies that observes five fields in separate parts of the sky in optical and near-infrared wavelengths.

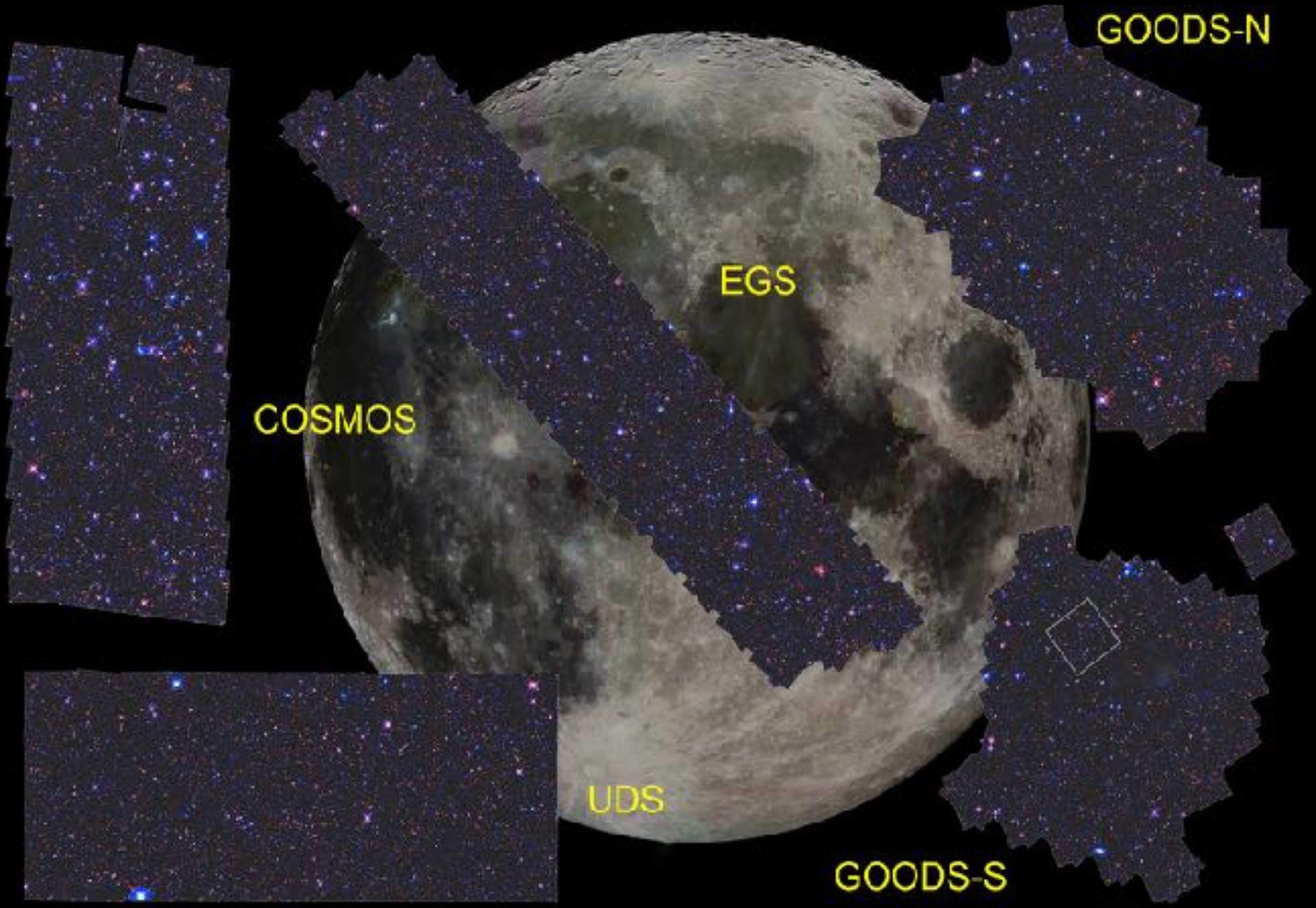

figure credit: the CANDELS team

UVCANDELS: the UV imaging of the CANDELS fields

- CANDELS is *Hubble*'s largest survey of distant galaxies that observes five fields in separate parts of the sky in optical and near-infrared wavelengths.
- UVCANDELS adds the blue-optical and UV images to four of these CANDELS fields with total sky coverage about 60% of that by the full moon.

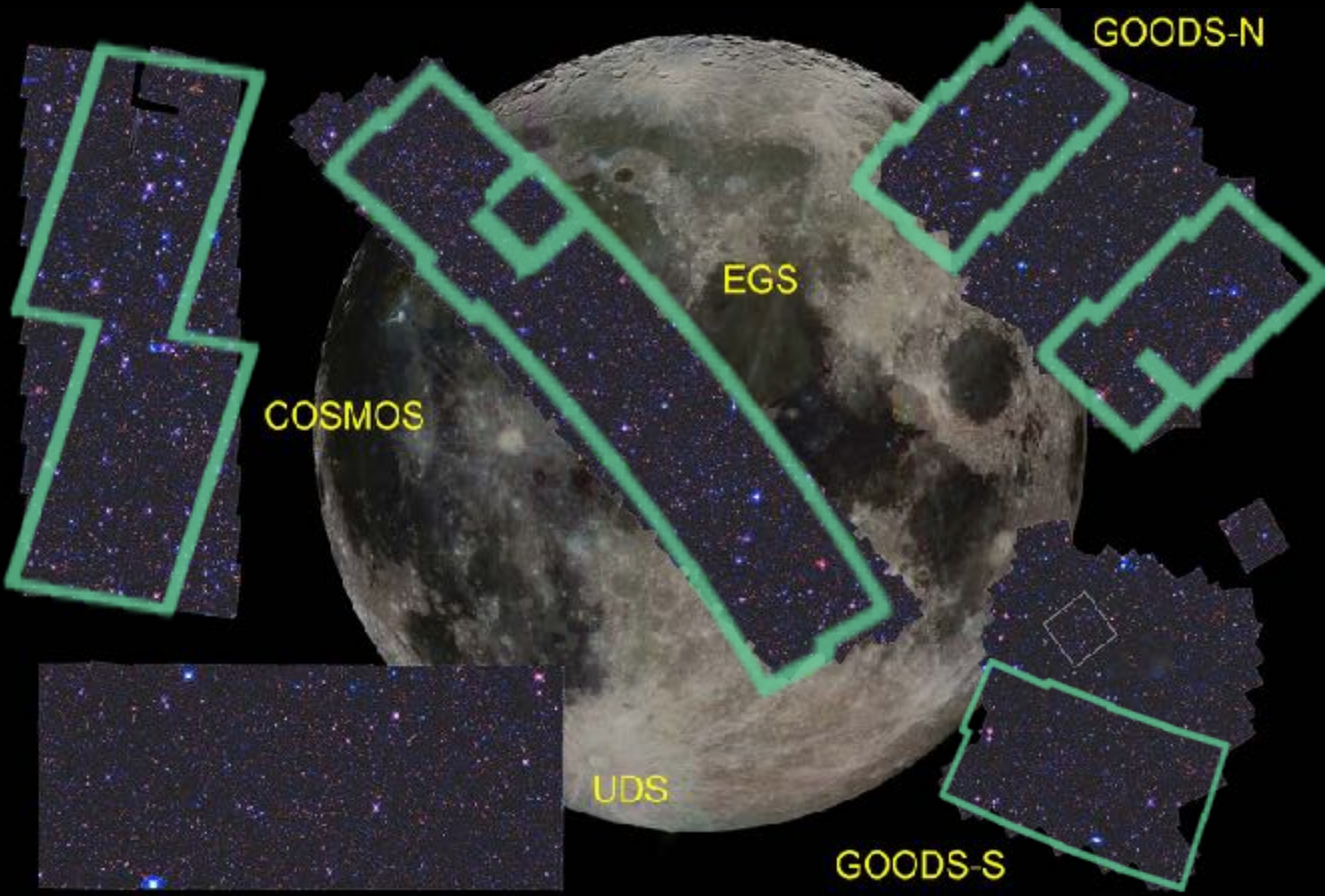

UVCANDELS UV footprints:

figure credit: the CANDELS team

The UVCANDELS Treasury Program

- Total area of UVCANDELS F275W imaging is **~430 arcmin²** (depth: 27 ABmag, 5-σ, r=0.2”), 2.5x larger than previous data combined!

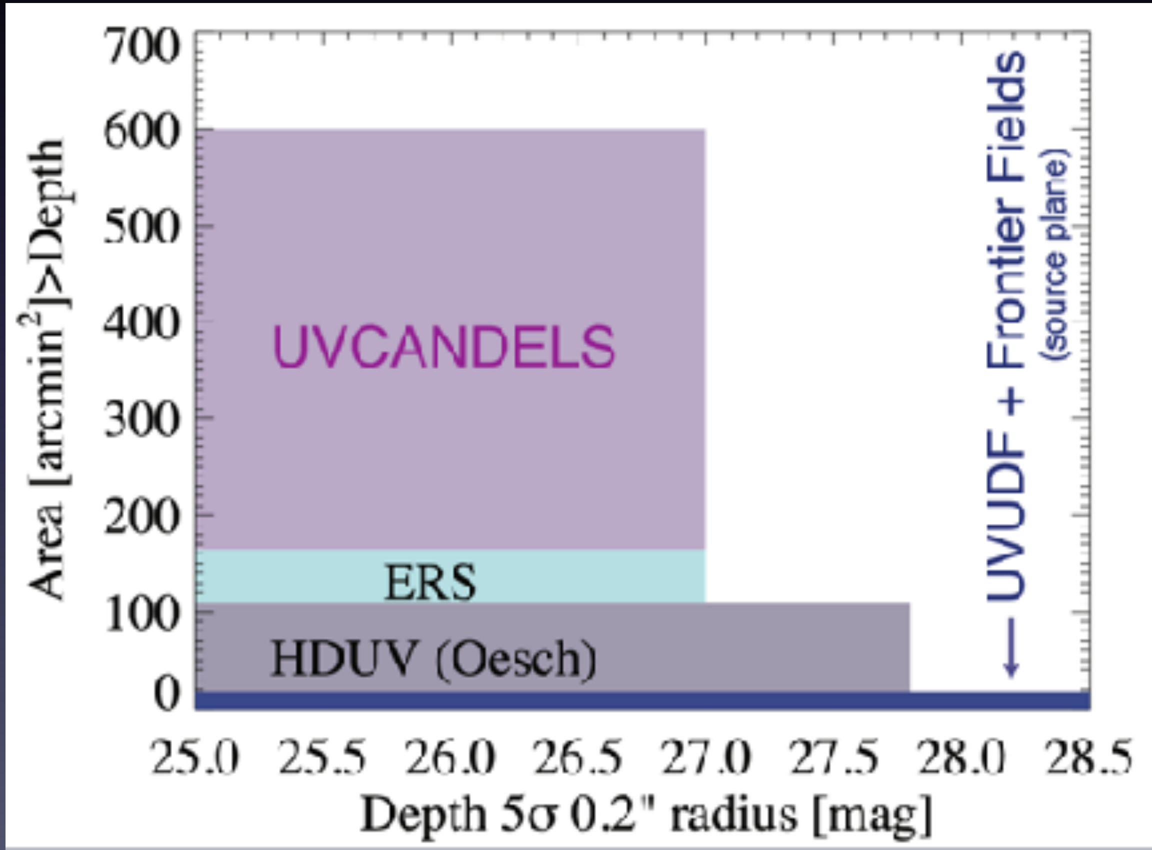

http://uvcandels.ipac.caltech.edu

The UVCANDELS Treasury Program

- Total area of UVCANDELS F275W imaging is **~430 arcmin²** (depth: 27 ABmag, 5-σ, r=0.2”), 2.5x larger than previous data combined!
- Measuring the escape fraction of the ionizing radiation (f_{esc}) is one of the major science goals of UVCANDELS.

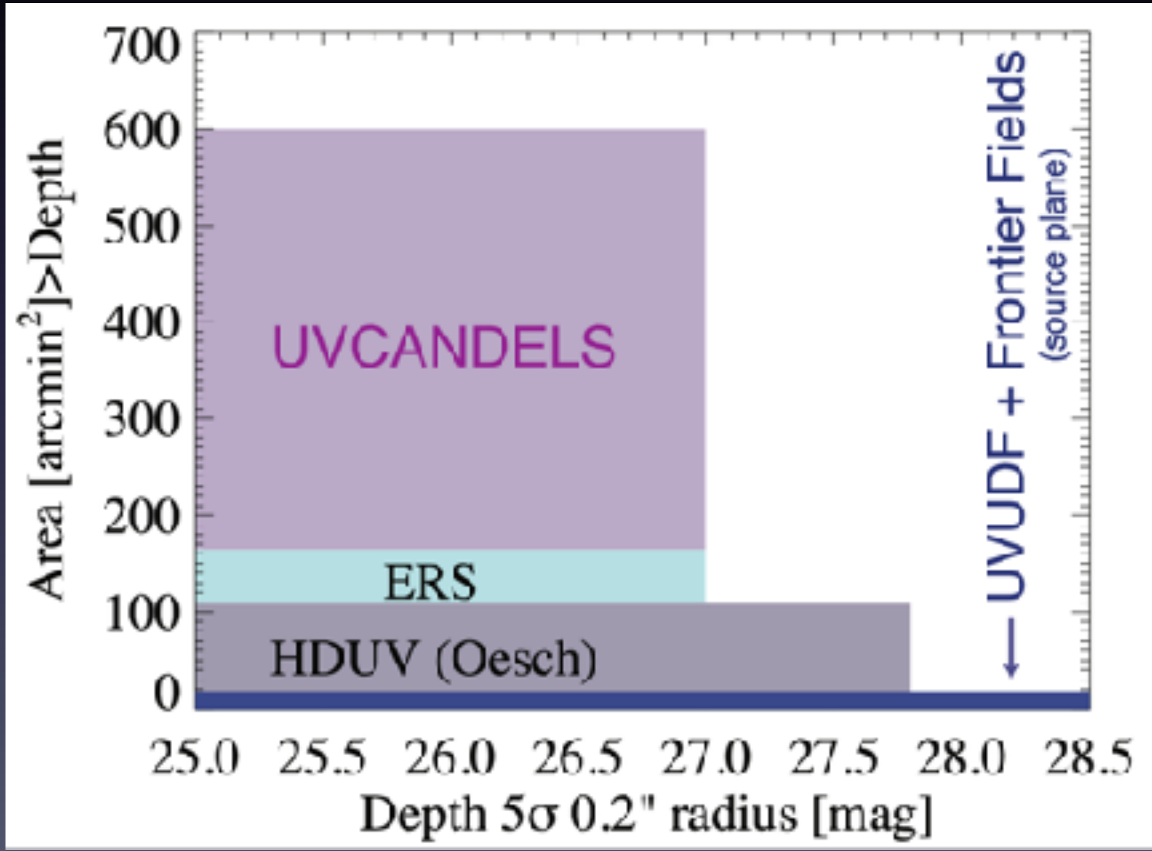

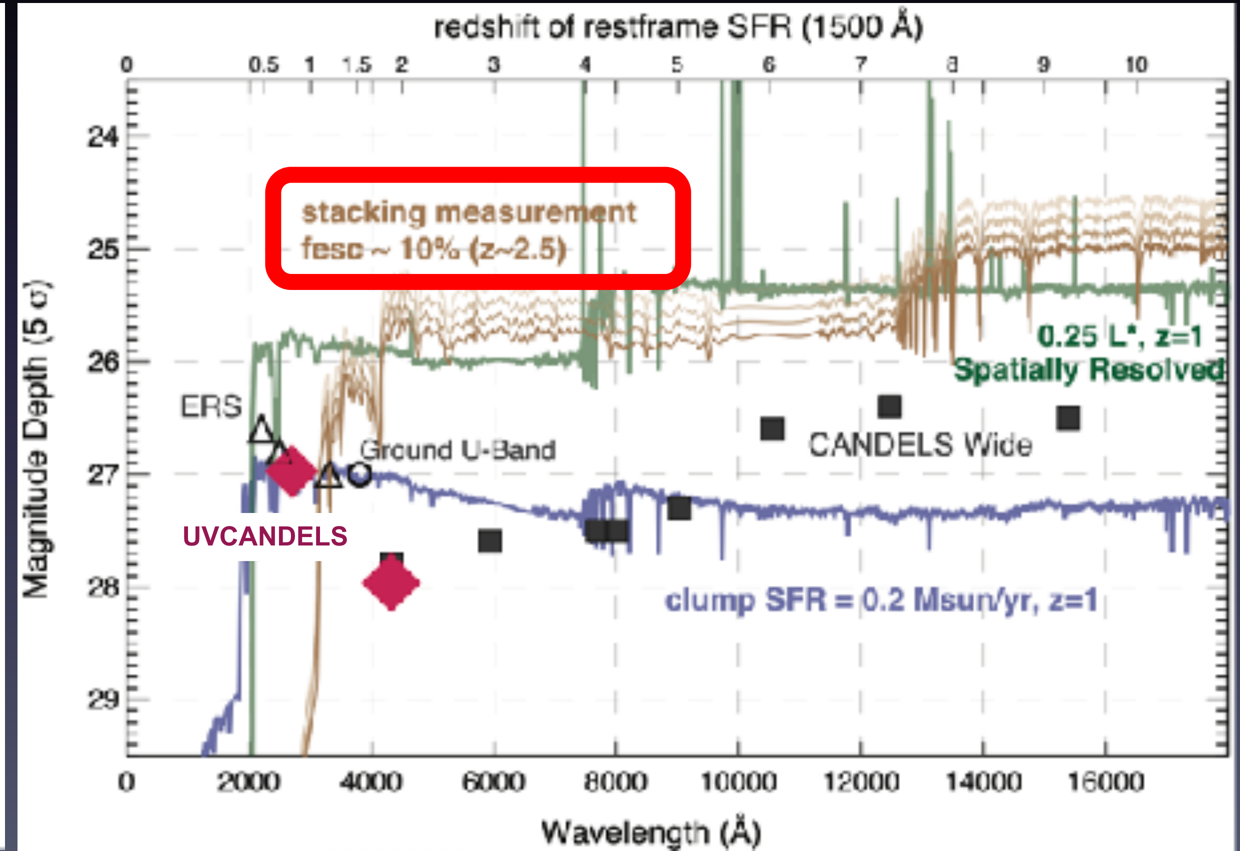

http://uvcandels.ipac.caltech.edu

Measuring the escape fraction of the ionizing radiation

- The ionizing radiation (at $\lambda_{rest} \leq 912$Å, a.k.a Lyman continuum, LyC) from star-forming galaxies is likely responsible for causing the cosmic reionization at $z \geq 6$, but it is not directly observable, b/c entirely absorbed by the highly neutral IGM.

Measuring the escape fraction of the ionizing radiation

- The ionizing radiation (at $\lambda_{rest} \leq 912$Å, a.k.a Lyman continuum, LyC) from star-forming galaxies is likely responsible for causing the cosmic reionization at $z \geq 6$, but it is not directly observable, b/c entirely absorbed by the highly neutral IGM.
- Relative f_{esc} : the ratio between the 1500Å and LyC photons intrinsically produced, divided by the ratio between them that escaped.

$$f_{esc,rel} = \frac{(f_{1500}/f_{LyC})_{int}}{(f_{1500}/f_{LyC})_{obs}} e^{\tau_{IGM}(z)}$$

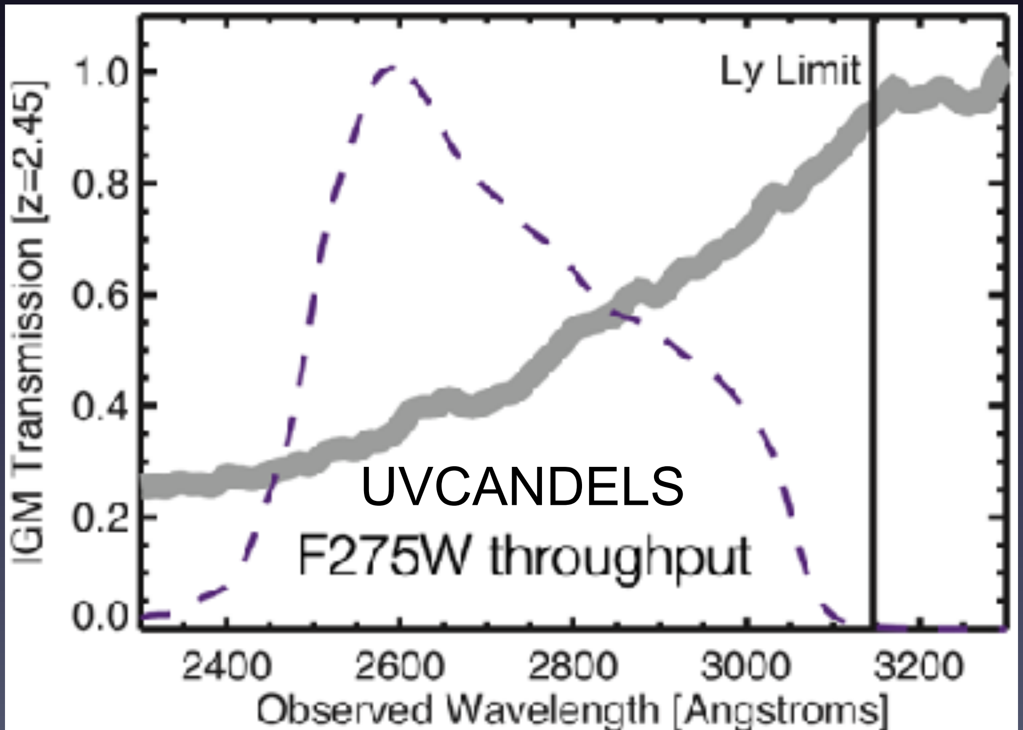

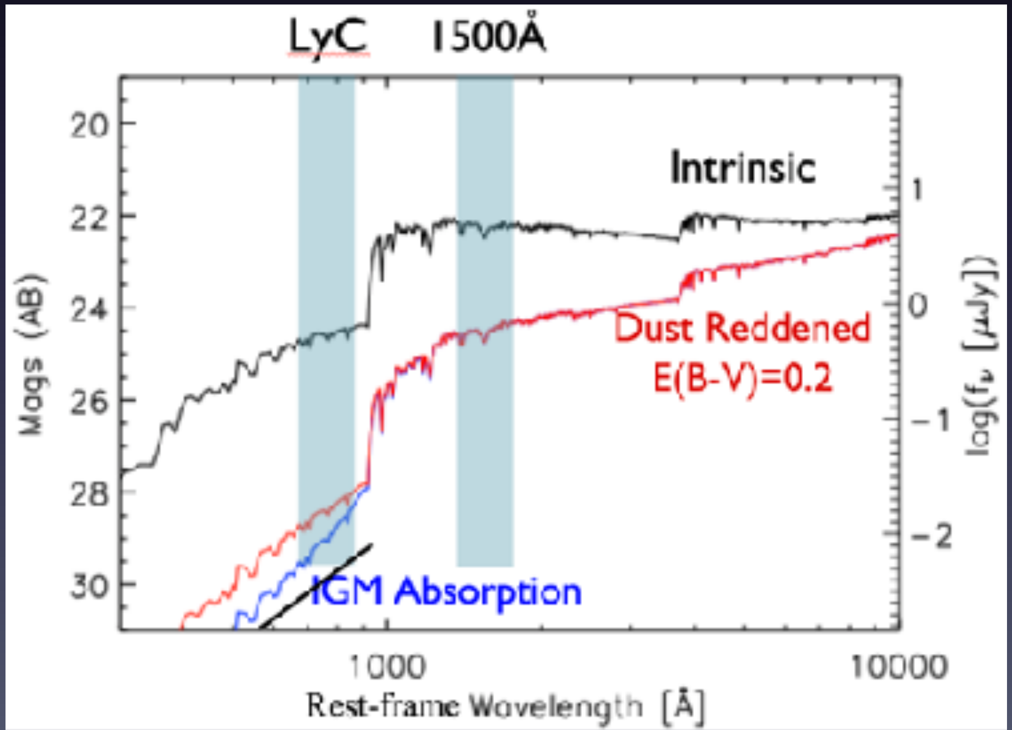

Measuring the escape fraction of the ionizing radiation

- using *potential* detections of individual galaxies and AGNs
- using the object stacking technique (following Siana+10, Rutkowski+16, Smith+18, 20)

=> improve detection limit, derive population average, divide into sub-groups

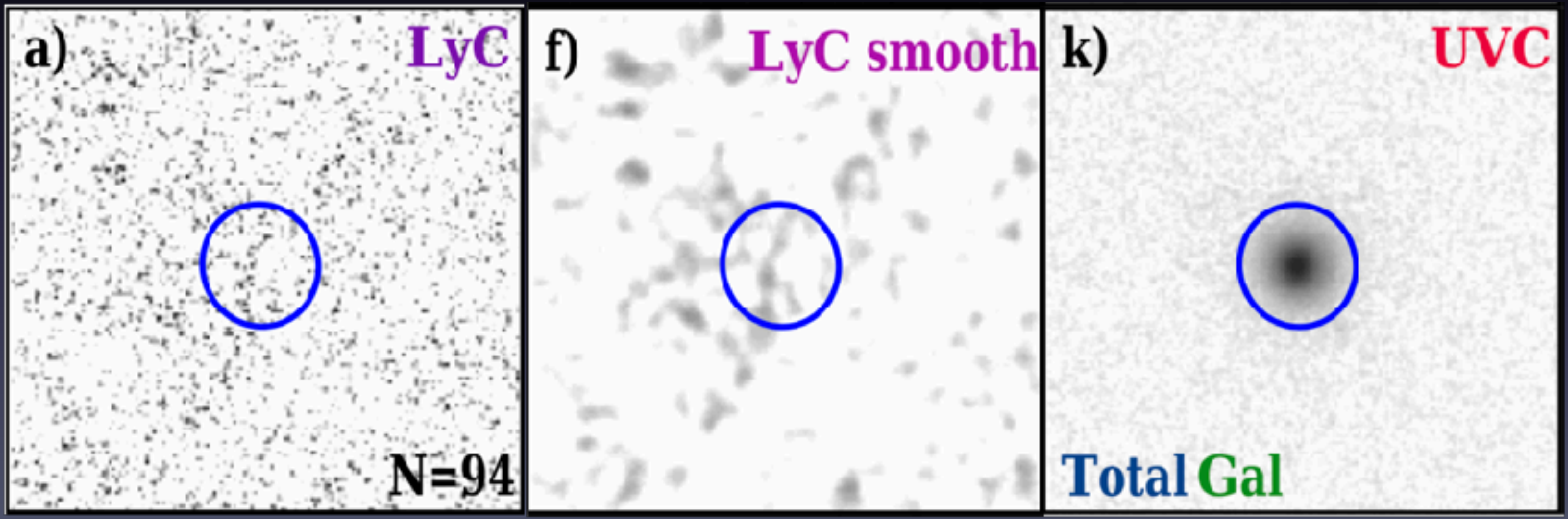

Smith+20

Basic procedures for the stacking analysis

1. Select sources with secure spec-z's
2. Make 30mas image cutouts in filters f275w, f435w, f606w, f814w
3. Create white light image for stamp photometry
4. Perform stamp photometry to find the centroid of source of interest and mask all other sources, also recenter the stamp
5. Visually inspect the RGB image and segmentation map from stamp photometry to further purify the stacking sample
6. Perform local background subtraction
7. Stacking via the inverse variance weighting method $\bar{f} = \frac{\Sigma(f_i/\sigma_i^2)}{\Sigma(1/\sigma_i^2)}, \quad \sigma^2 = \frac{1}{\Sigma(1/\sigma_i^2)}$
8. Perform photometry on the stacked images
9. Separate all sources into different groups and redo stacking

Stacking results: the full sample (N_{gal}=102)

- all galaxies that have secure spectroscopic redshifts at $z \geq 2.4$

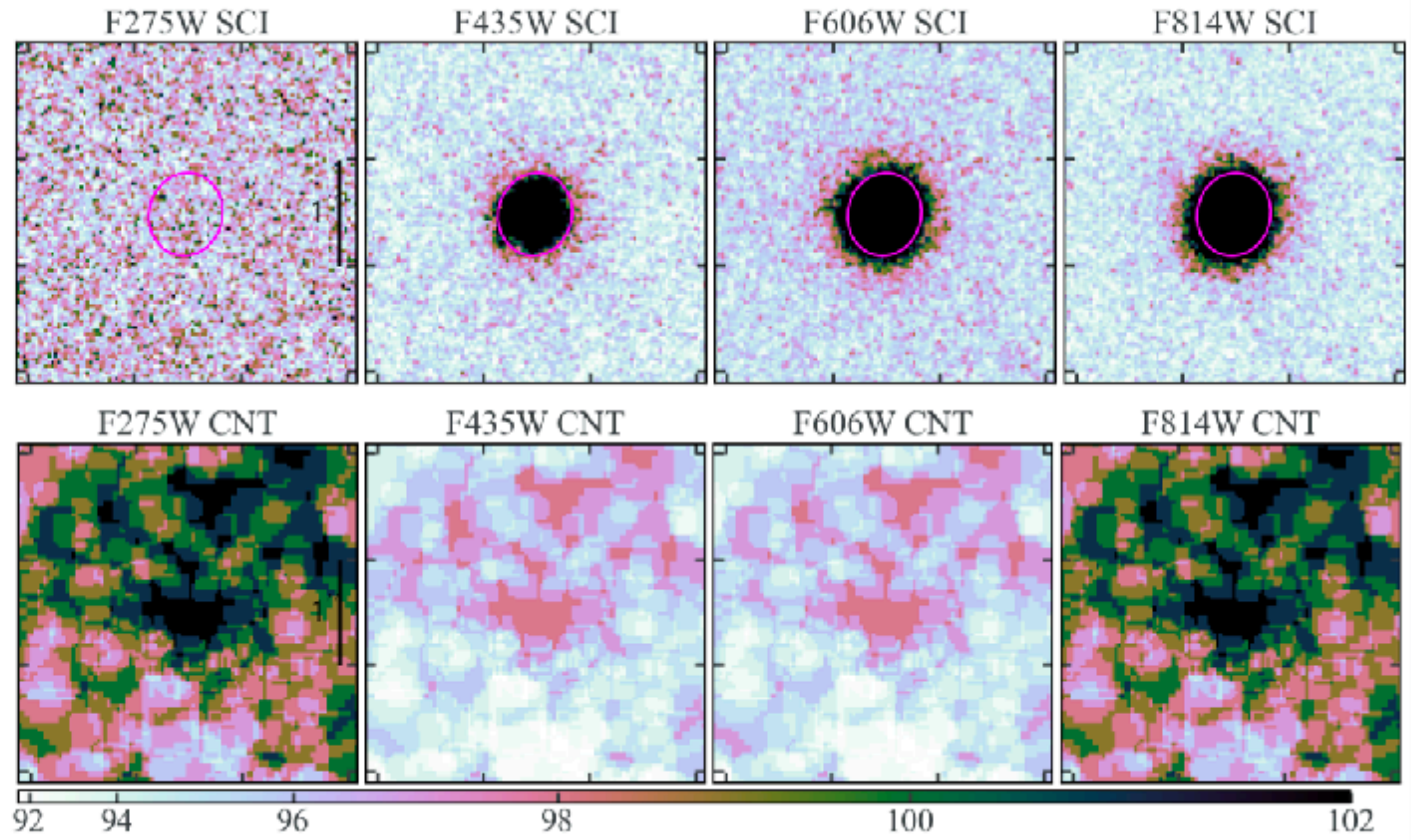

Wang et al. (2022c) in prep.

Stacking results: the full sample (N_{gal}=102)

- f275w mag = 29.48+/-0.39, SN=2.78 => fesc,rel = 6.5%
- offsets btw the peaks of LyC and UVC => support the clumpy ISM geometry with non-uniform covering fraction conducive to LyC leakage

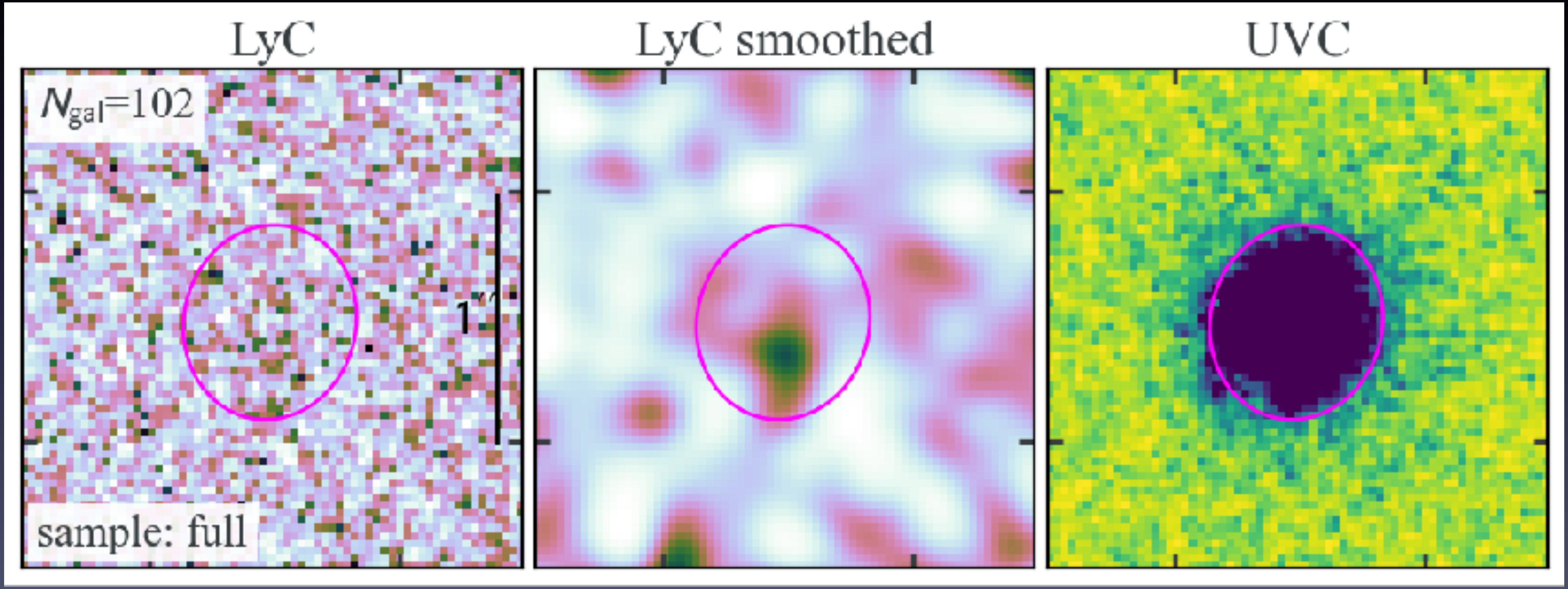

Wang et al. (2022c) in prep.

Stacking results: the snO2 sample (N_{gal}=34)

- f275w mag = 29.00+/-0.30, SN=3.56 => fesc,rel = 18.4%
- strong emission-line galaxies are predominant in driving the cosmic reionization and maintaining the UV ionization background

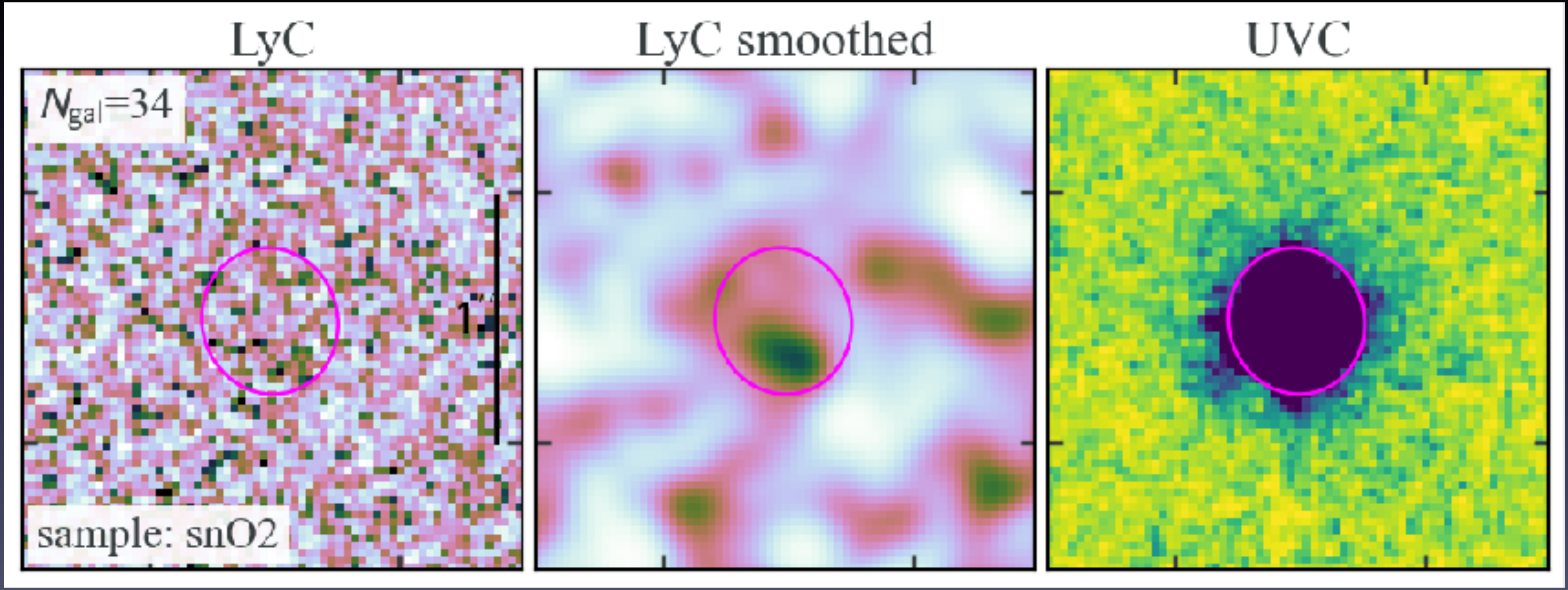

Wang et al. (2022c) in prep.

Part I: Space-based Wide-field Slitless Spectroscopy

Part II: Space-based Near-Ultraviolet Imaging

Part III: Prospect for our CSST Main Survey

CSST主巡天探测器排布与观测方案

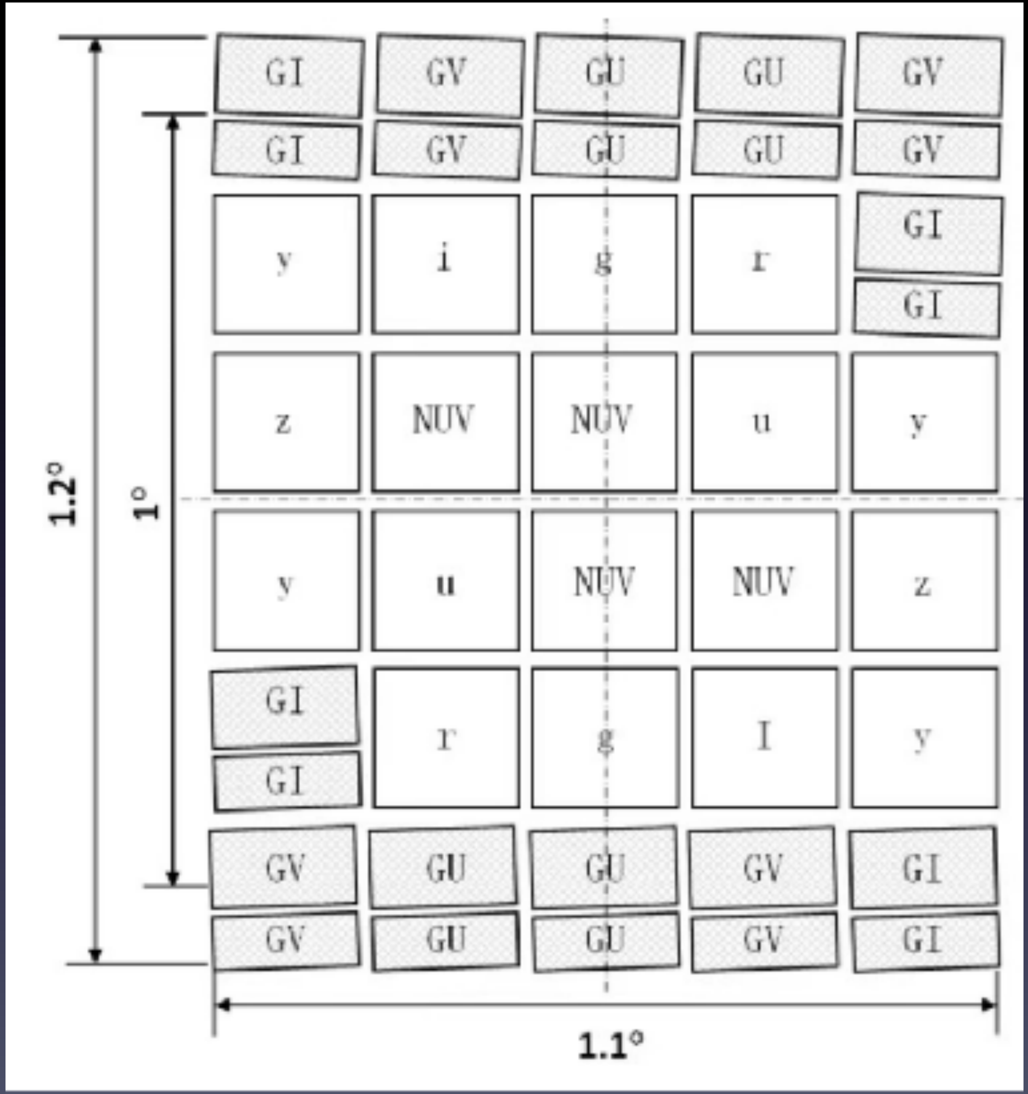

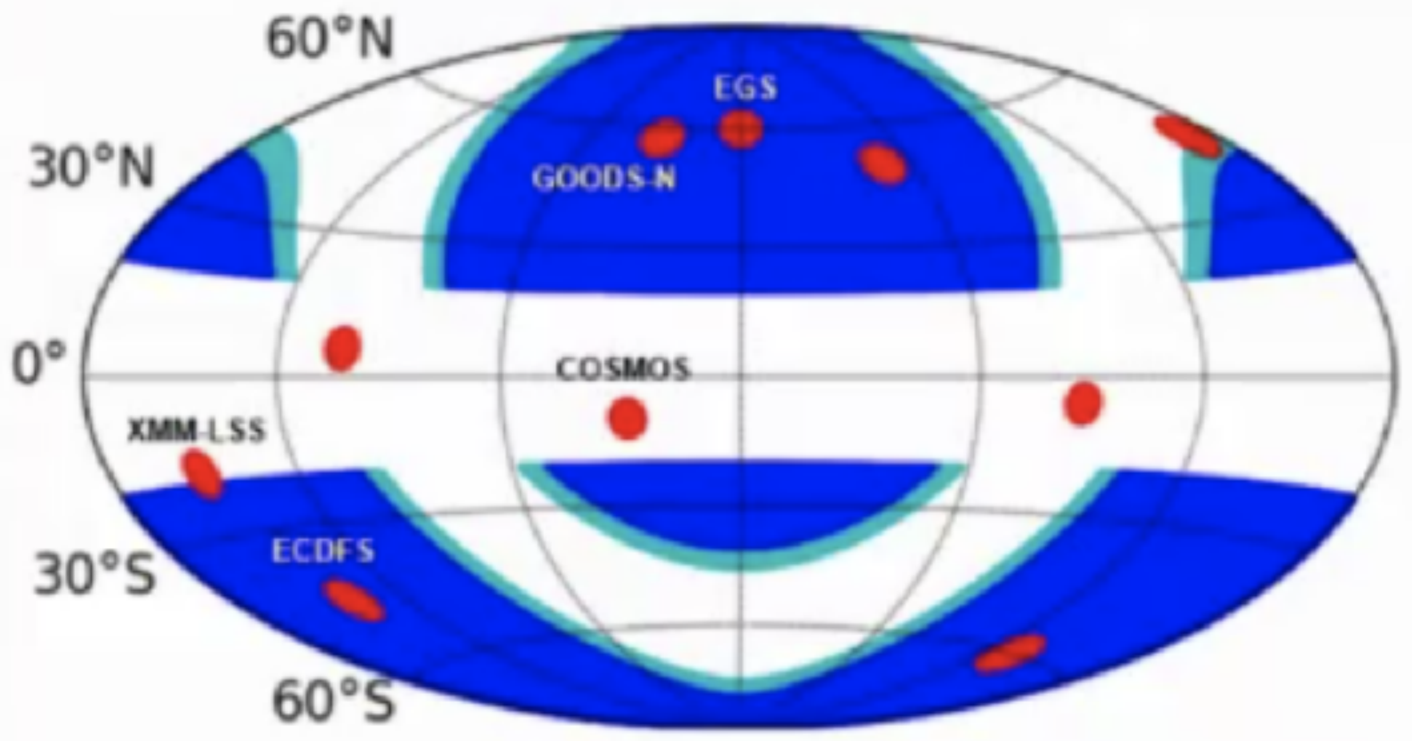

17500□°多色成像：255-1000nm，≥6 滤光片，平均≥25.5等

17500□°无缝光谱：255-1000nm，λ/Δλ ≥200，≥20-21ᵐ/res

400□°深场：多色成像+无缝光谱，比大面积观测深1星等以上

300□′超深场(MCI)：同时、同视场三色分光，V ≥ 30等

CSST主巡天极限星等与波长覆盖

	t_{exp}	GU	GV	GI
17500□°	4×150s	20.5	21.0	21.0
400□°	16×250s	21.8	22.2	22.1

	t_{exp}	NUV*	u	g	r	i	z	y*
17500□°	2×150s	25.4	25.4	26.3	26.0	25.9	25.2	24.4
400□°	8×250s	26.7	26.7	27.5	27.2	27.0	26.4	25.7

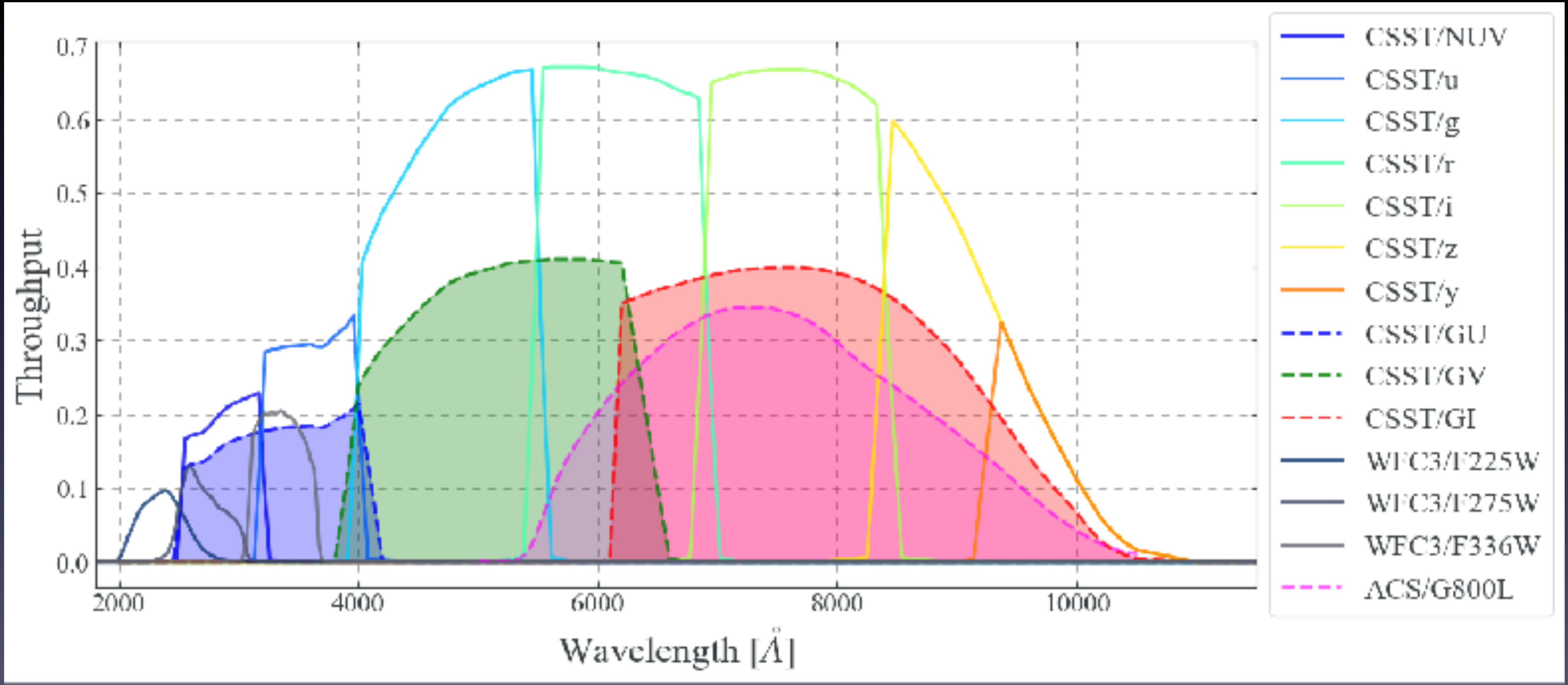

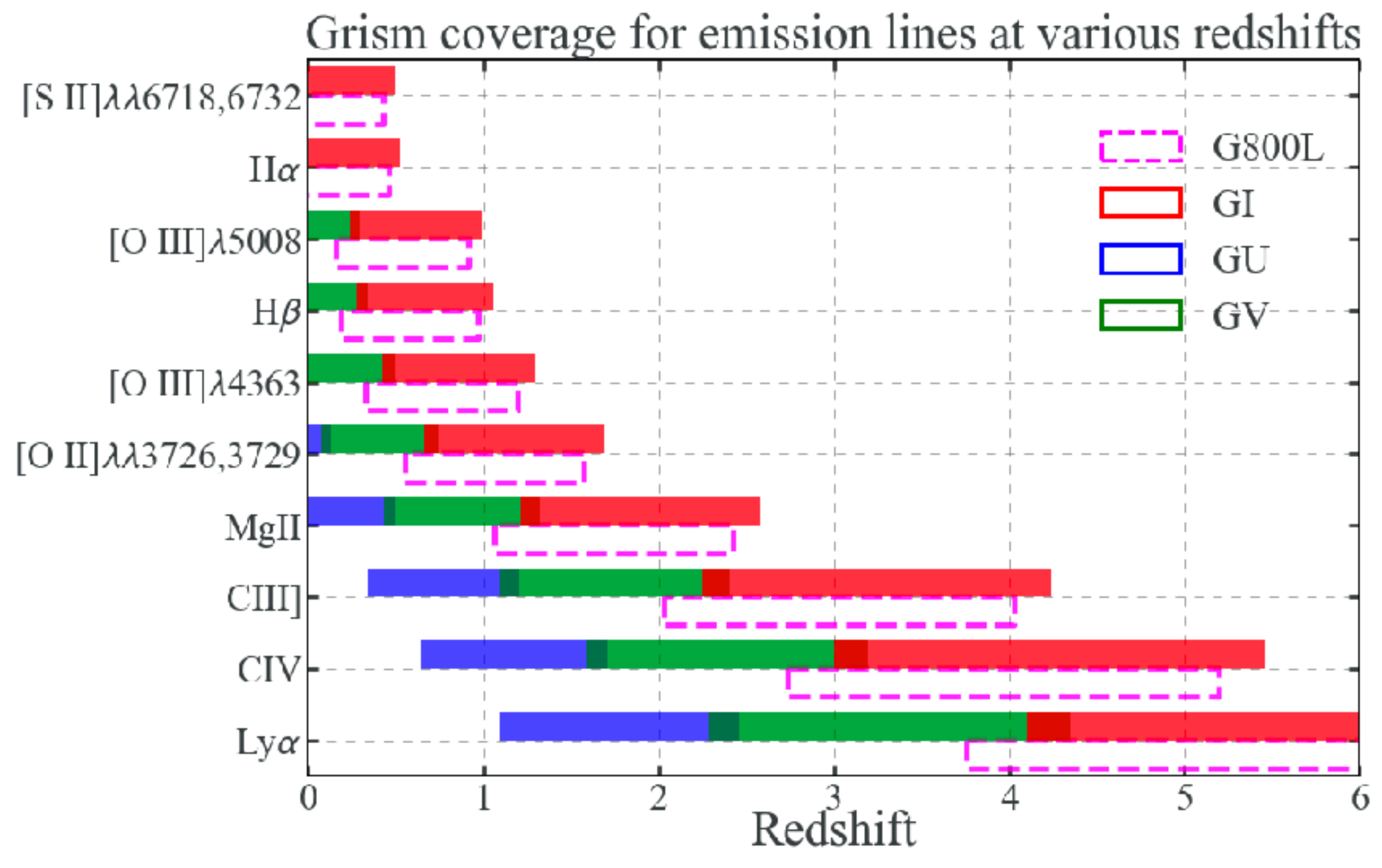

Grism coverage for emission lines at various redshifts
[S II]λλ6718,6732
Hα
[O III]λ5008
Hβ
[O III]λ4363
[O II]λλ3726,3729
MgII
CIII]
CIV
Lyα
G800L
GI
GU
GV
0
1
2
3
4
5
6
Redshift

CSST无缝光谱红移测量初步结果

input source: a quasar at z_input = 0.775, z_fit = 0.736 +/- 0.007 (3-sigma)

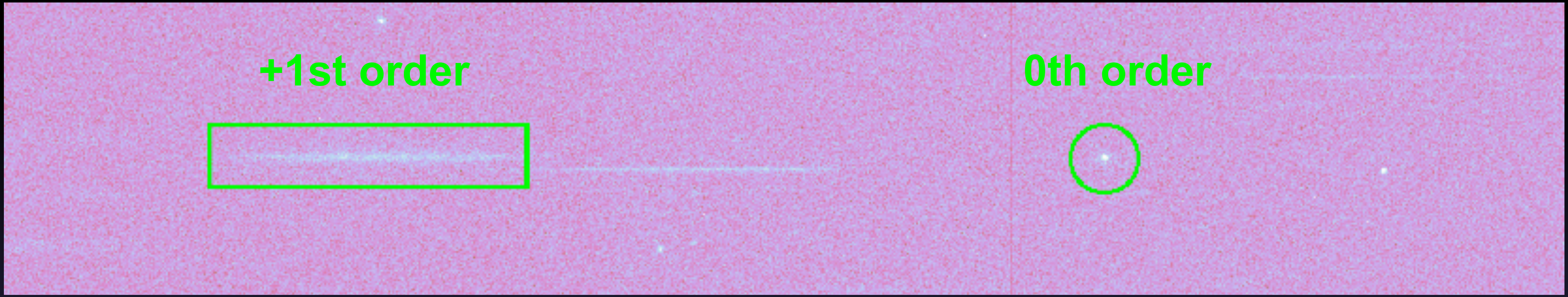

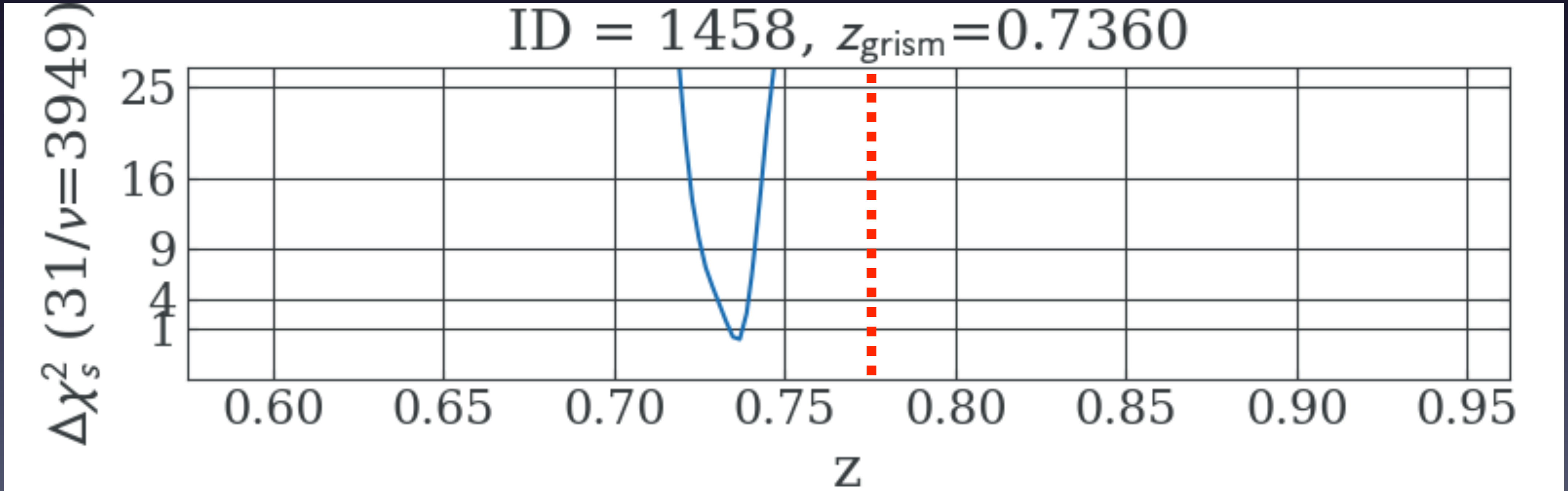

无缝光谱数据单独红移拟合

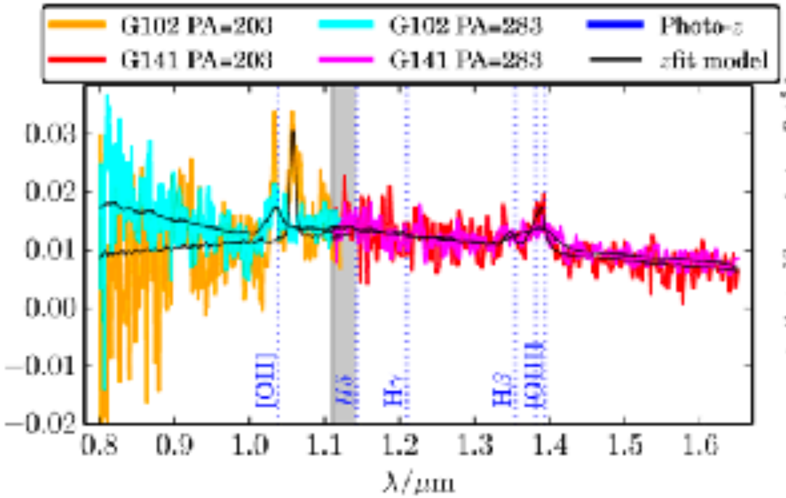

无缝光谱与宽波段测光数据联合红移拟合

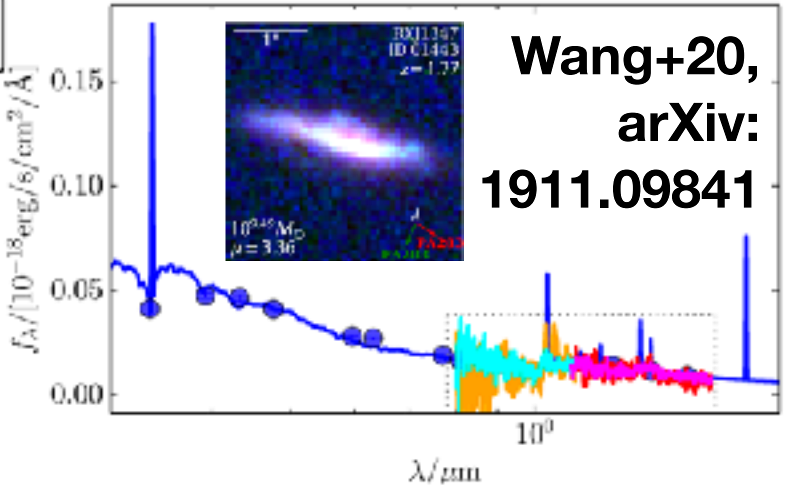

对红移参数限制的后验概率

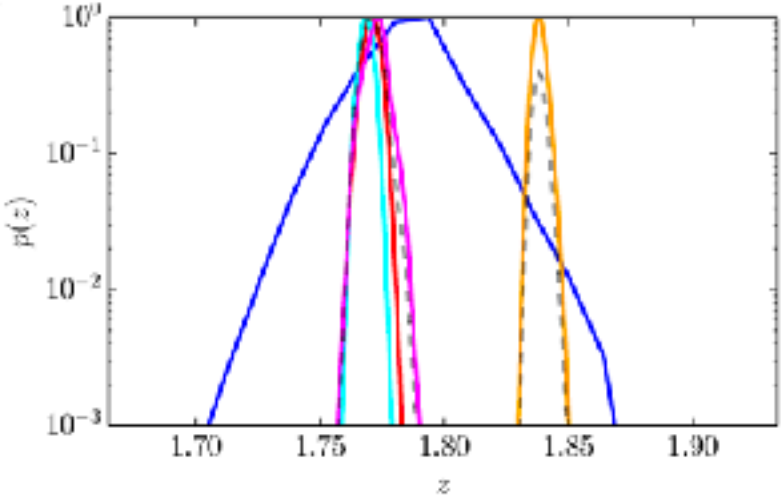

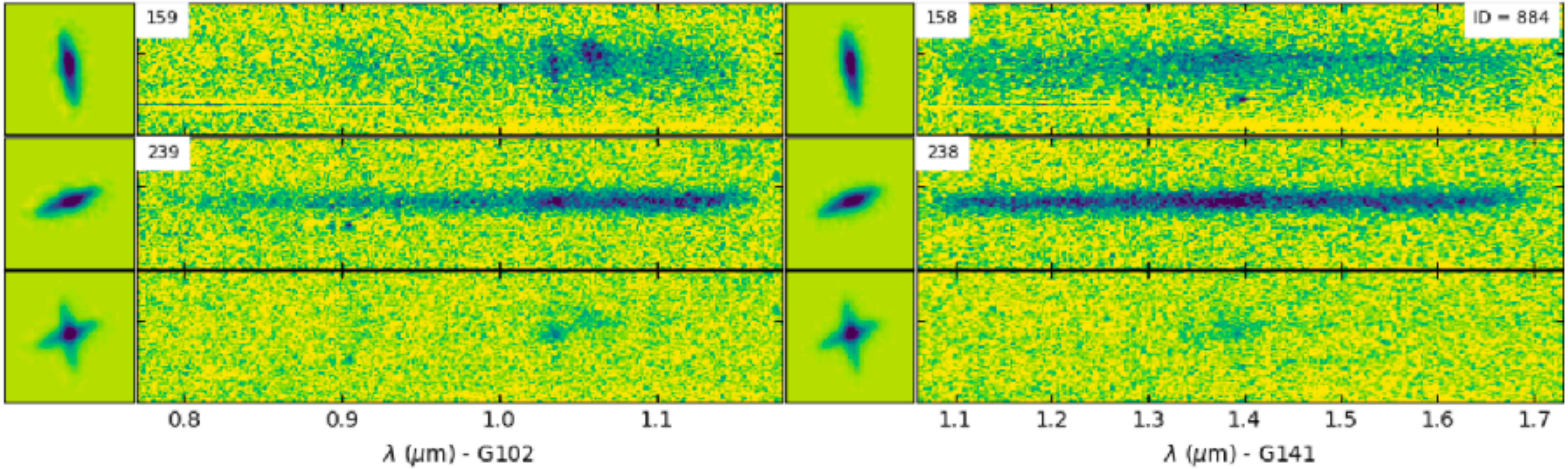

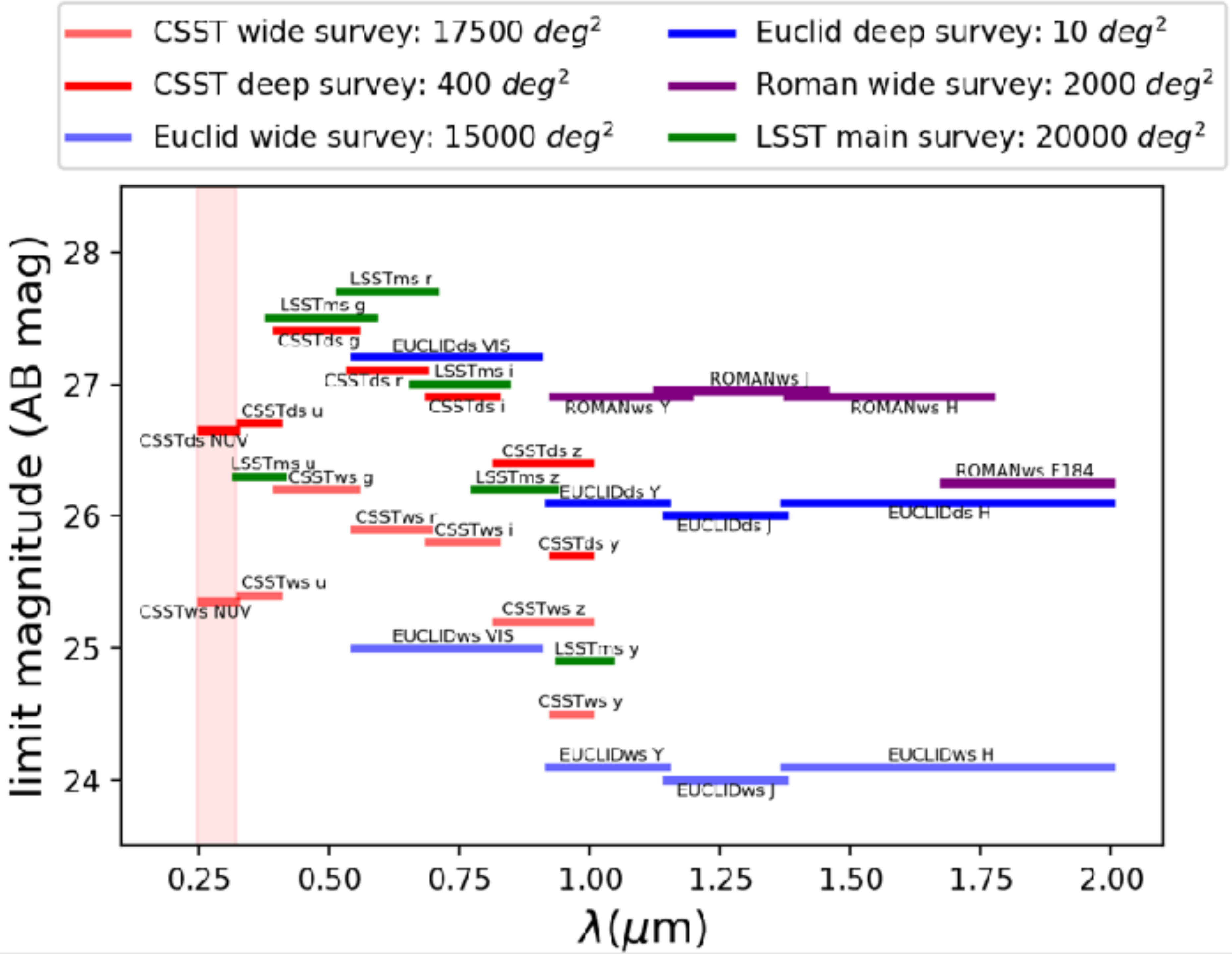

CSST wide survey: 17500 deg^2
CSST deep survey: 400 deg^2
Euclid wide survey: 15000 deg^2
Euclid deep survey: 10 deg^2
Roman wide survey: 2000 deg^2
LSST main survey: 20000 deg^2
limit magnitude (AB mag)
$\lambda(\mu m)$
0.25
0.50
0.75
1.00
1.25
1.50
1.75
2.00
24
25
26
27
28
LSSTms r
LSSTms g
CSSTds g
EUCLIDds VIS
CSSTds r
LSSTms i
CSSTds i
ROMANws J
ROMANws Y
ROMANws H
CSSTds u
CSSTds NUV
CSSTds z
LSSTms u
CSSTws g
LSSTms z
EUCLIDds Y
ROMANws F184
EUCLIDds J
EUCLIDds H
CSSTws r
CSSTws i
CSSTds y
CSSTws u
CSSTws NUV
CSSTws z
EUCLIDws VIS
LSSTms y
CSSTws y
EUCLIDws Y
EUCLIDws H
EUCLIDws J

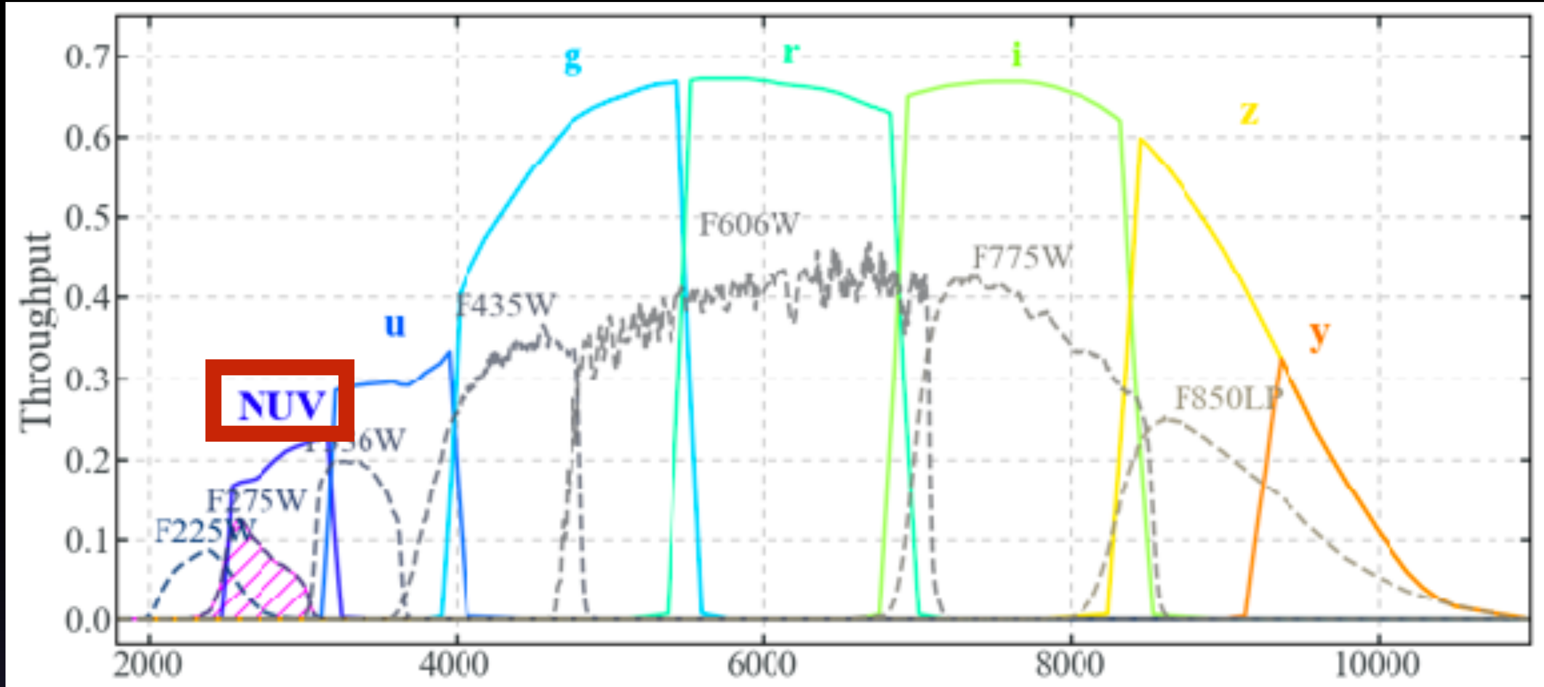

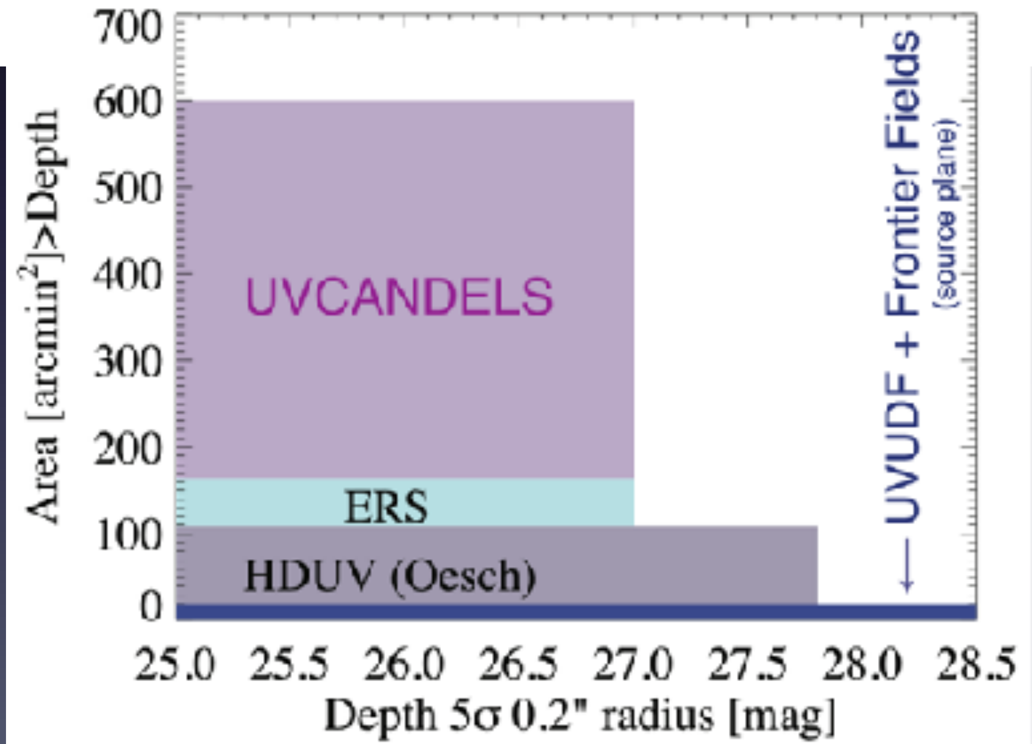

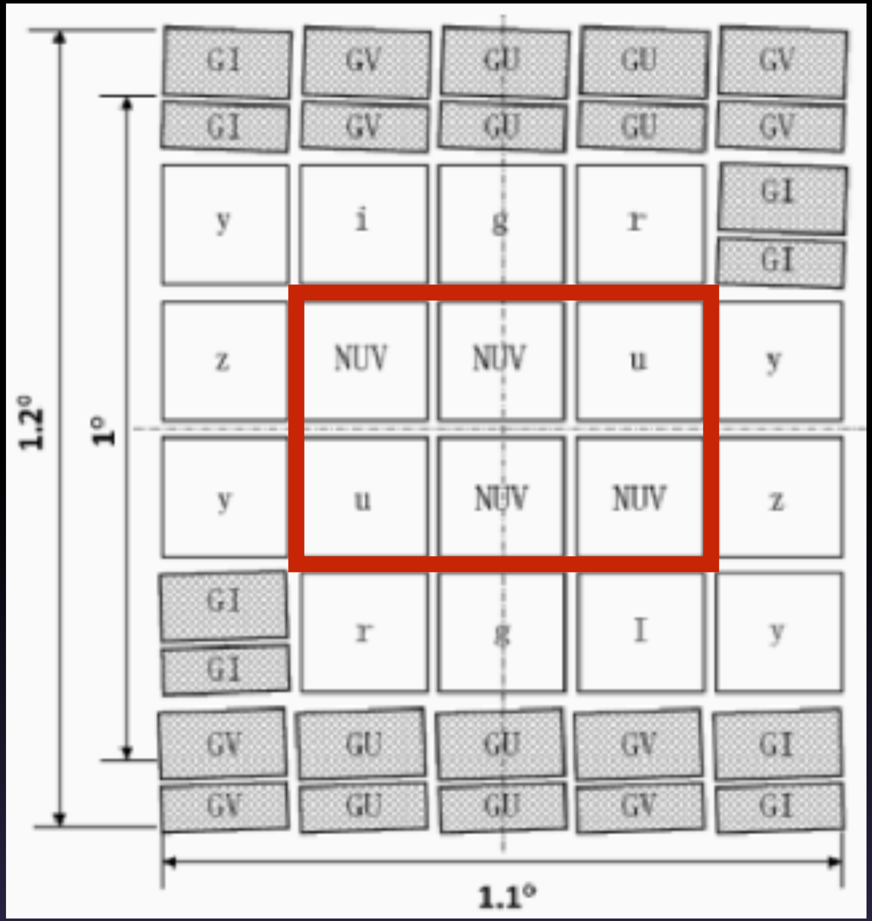

- CSST/NUV (from Zhan 2021)
  - lim. mag: 26.7 (25.4)
  - exp. time: 250x16 (150x4) sec
  - survey area: 400 (17500) sq. deg
  - ang reso (R80): 0.135 arcsec

Improved aperture photometry method

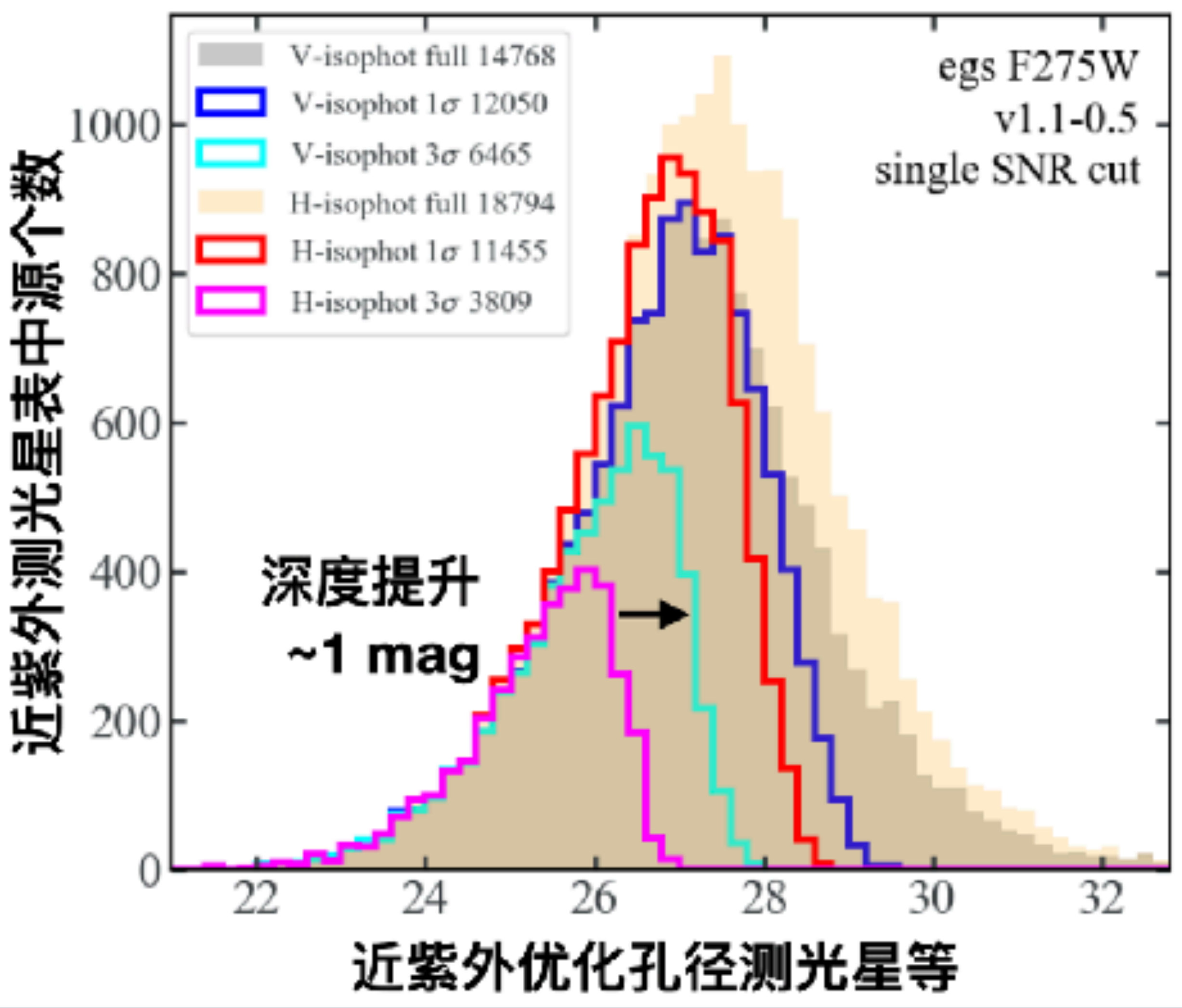

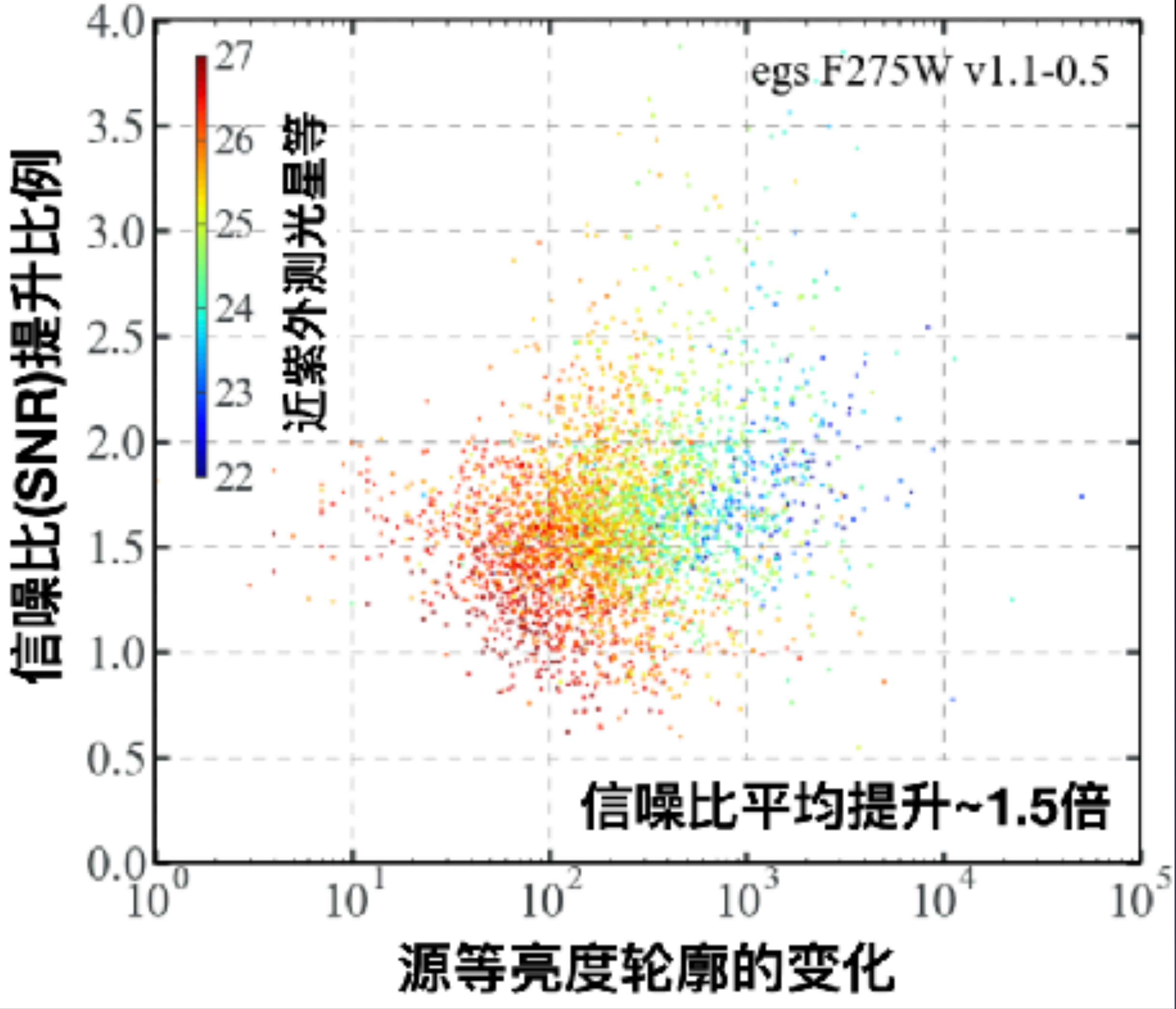

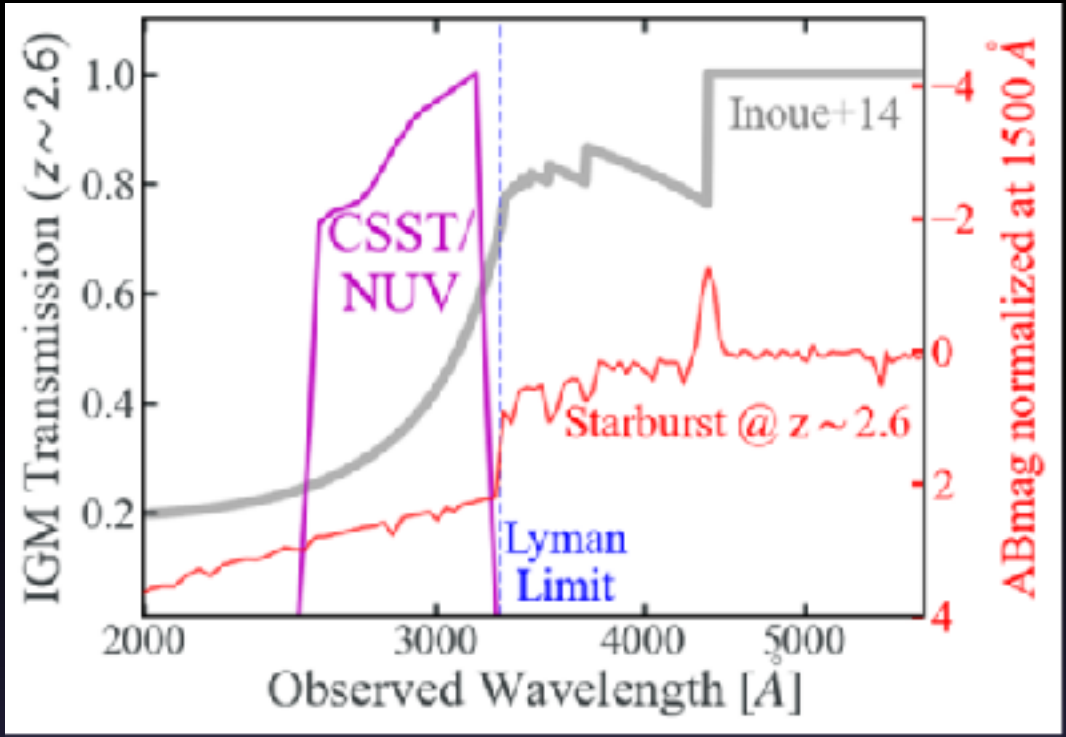
IGM Transmission ($z \sim 2.6$)
1.0
0.8
0.6
0.4
0.2
2000
3000
4000
5000
Observed Wavelength [Å]
ABmag normalized at 1500 Å
−4
−2
0
2
4
Inoue+14
CSST/
NUV
Lyman
Limit
Starburst @ z ~ 2.6

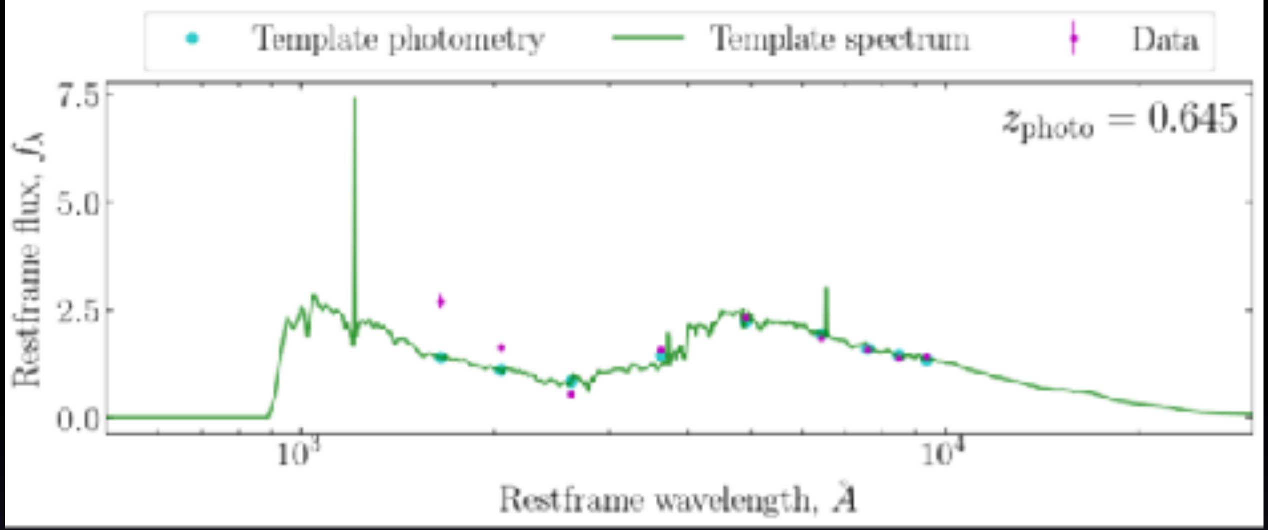
Template photometry
Template spectrum
Data
$z_{\rm photo} = 0.645$
Restframe flux, f_λ
7.5
5.0
2.5
0.0
10^3
10^4
Restframe wavelength, Å

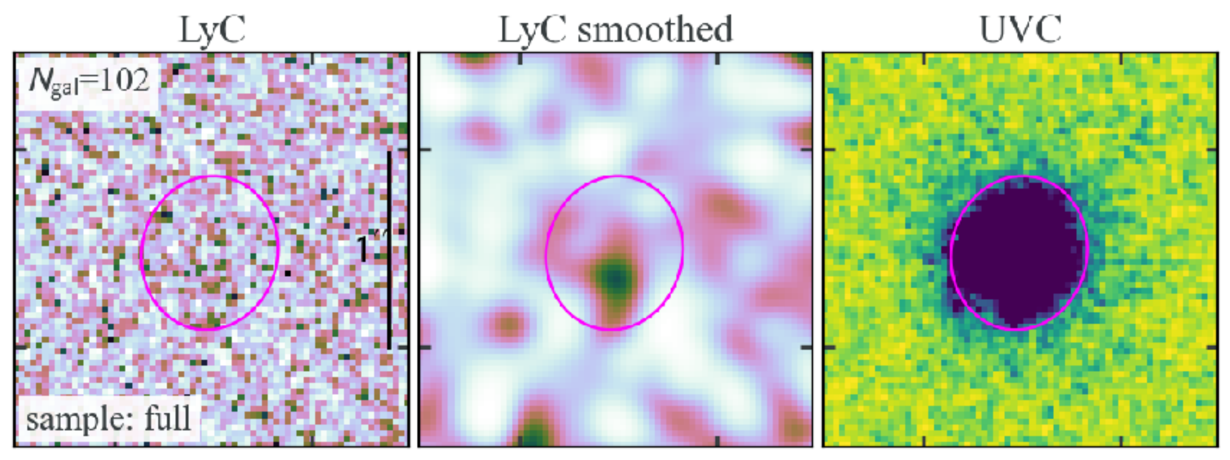
LyC
LyC smoothed
UVC
$N_{\rm gal}$=102
1″
sample: full

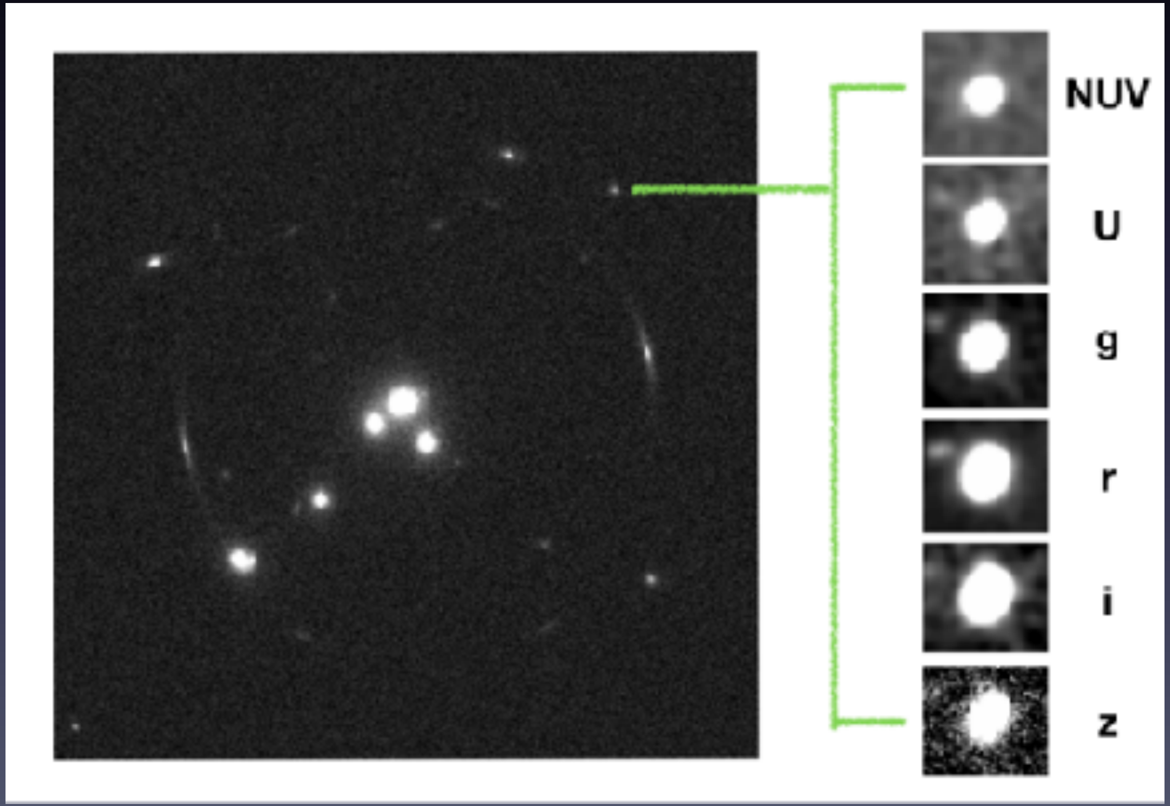
NUV
U
g
r
i
z

Thanks for your attention!